Indian Journal of Pure & Applied Physics
Vol. 61, April 2023, pp. 268-290
DOI: 10.56042/ijpap.v61i4.69622

A Historical Review of Electrode Materials and Electrolytes for Electrochemical Double Layer Supercapacitors and Pseudocapacitors

Parveen Saini*

Conducting Polymers, Graphene Technology and Waste Management Group, Photovoltaic Metrology Section, Advance Materials and Devices Metrology Division, CSIR-National Physical Laboratory, Dr. K.S. Krishnan Marg, New Delhi 110 012, India

Received 15 December 2022; accepted 27 March 2023

The supercapacitor is one of the most promising alternatives to other popular energy storage solutions, viz., rechargeable batteries and capacitors. They are considered the bridge between batteries (high energy density) and capacitors (high power density) because of their fast charge/discharge capacity, high specific power/energy, and good service-life, which make them the most promising candidate for future energy storage/redistribution systems as well as hybrid electric vehicles. In the past, much progress has occurred in electrode materials, electrode architecture, electrolytes, separators, and device configuration. This review article discusse the basics of electrochemical super capacitors, storage principal, device configuration, electrode materials, and electrolytes, including the coverage of the comprehensive literature account of the advancements in the area; and, finally, the discussion on technological challenges in the development of commercially viable next-gen supercapacitor devices.

Keywords: Supercapacitor; Ultracapacitor; Electrochemcial double layer capacitor (EDLC); Pseudocapacitor; Activated carbon; Carbon nanotubes (CNTs); Carbon aerogel; Graphene; Conducting polymer; Polyaniline; Polypyrrole; Polythiophene; Hybrid supercapacitors; Energy density; Power density; Ragone plot

1 Introduction

The rapid depletion of fossil fuels, climatic changes, and growing energy demands have encouraged researchers to seek efficient energy harvesting and storage solutions based on renewable resources and environment-friendly technologies[1–5]. Notably, the R&D initiatives related to developing devices for efficient storage have gained momentum to satisfy the needs of portable electronics, electric vehicles, and heavy-duty equipment or machines[1,6–12]. Two important classes of conventional energy storage devices are electrochemical batteries (*e.g.*, lead acid, Ni-Cd, or Li-ion type secondary batteries) and electrostatic capacitors (*e.g.*, metal oxide or conducting polymer electrolyte-based capacitors)[13–18]. Batteries display high energy density and good service life with economic feasibility but suffer disadvantages like low specific power, slow charging, and safety issues. Similarly, capacitors exhibit high power density, low charging time, stable operation, and compactness with low energy density as a severe drawback that restricts their utility only for low-power applications such as analog circuit components, short-term memory backup systems, *etc*.[13,19]. Recently, supercapacitors (SCs), also known as ultracapacitors, have emerged as the most powerful and promising alternative for state-of-the-art electrical energy storage and delivery systems[13,14,20].Compared to batteries and capacitors, SCs occupy an essential position (Fig. 1) concerning power output and energy storage capacity regarding energy density versus power density graphs, popularly known as Ragone plots[21]. SCs tend to display the high energy density of batteries and the high power density of capacitors. In other words, they are lightweight compared to the battery of the same power storage capacity (high power density), give fast access to the stored energy (sustain high discharge rates) and display low charging times (few minutes or even seconds) while possessing higher energy holding capacity compared to equivalent size/weight capacitor (high energy density)[13,19,19,21–23]. However, technological limitations make SCs relatively expensive compared to batteries or capacitors. The continuedprogress in SCs and the emergence of nanotechnology has changed the scenario with the evolution of capabilities of synthesizing controlled porosity, desired wettability characteristics, low resistance, and large surface area materials for enhancing the charge storage capacity[21–23].

*Corresponding author: (E-mail: pksaini@nplindia.org)

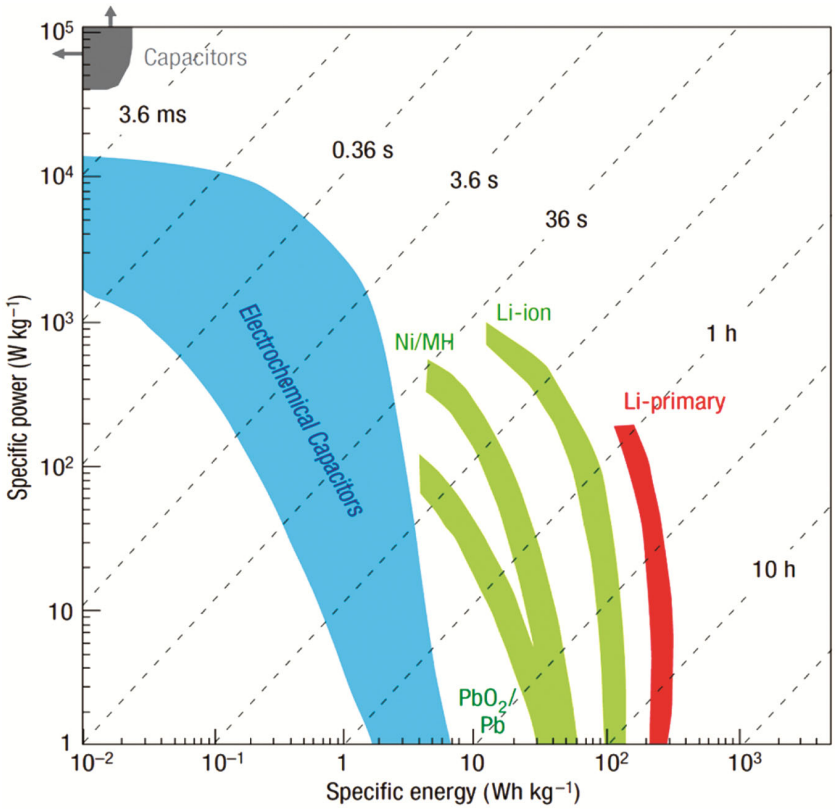

Fig. 1 — Ragone plot of different energy storage devices viz. conventional capacitors, batteries and supercapacitors[21], (Reprinted with the permission).

Table 1 — Comparison of different properties of various energy storage systems.

Parameters	Capacitor	Supercapacitor	Battery
Charging time (s)	10^{-6} to 10^{-3}	1 to 30	1000 to 10000
Discharge time (s)	10^{-6} to 10^{-3}	1 to 30	3000 to 15000
Specific energy (Wh/kg)	0.1 or less	5 to 10	25 to 100
Specific power (kW/kg)	0.25 to 10000	10 to 100	0.005 to 0.4
Cycle life (number of charge-discharge cycles)	>500000	>100000	500 to 2000
Coulombic efficiency	1.0	0.90 to 0.95	0.70 to 0.85

Table 1 lists the detailed comparison between the battery, capacitor, and supercapacitor in terms of parameters and typical values. As stated earlier, it is evident from the data that with moderate values of specific energy and power, SCs fill the gap between high-energy-density devices like secondary batteries and high-power-density devices like capacitors.[13,21,23]. They can store hundreds or thousands of times more charge than conventional capacitors (Table 1) because of a much larger surface area for charge storage (the reason for high energy density). Further, they can also rapidly release the stored charge in a controlled manner (reason for high power density)[14]. Therefore, SCs can complement the battery in terms of specific power or capacitor in terms of specific energy, thereby enabling optimized energy and output power realization.

2 Historical Background

The charge storage phenomenon at the metal/electrolyte interface has been known since the 19th century. However, it was only in 1957, *i.e.*, upon granting of the very first patent on a supercapacitor based on highly porous carbon electrodes (Fig. 2: originally patented supercapacitor device), to Becker and co-workers of GE Corporation[24], when the double-layer capacitors started finding practical applications.

Later, the SOHIO patented a modified SC in 1966, exploiting high surface area carbon as the active

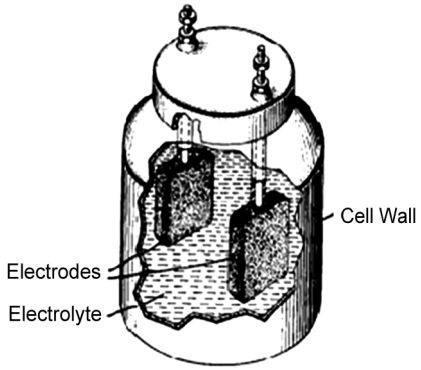

Fig. 2 — The capacitor patented by M/S General Electric Corp[24].

electrode and tetra alkyl ammonium salt-based electrolyte[25]. In 1970, they patented a circular disc capacitor comprising carbon paste soaked in an electrolyte[26]. Later, SOHIO NEC took the technology in 1971 and produced the first commercial double-layer capacitor device called a "supercapacitor" [27]. Due to their low output voltage and high internal resistance, their primary application was memory backup and portable electronics. Later, B. E. Conway and co-workers[13,14,20,28] extended significant contributions towards the development of supercapacitor technology, particularly based on transition metal oxides (*e.g.*,RuO_2),which display high specific capacitance and low internal resistance resulting in good power output. In the 1990s, for applications in hybrid electric vehicles (HEVs),SCs were extensively explored. Currently, the commercially viable SC devices are primarily based on high specific surface area porous carbon materials and metal oxides[21–23]. Later, MEI (Panasonic, Japan) designed Gold capacitors, whereas Pinnacle Research (USA) developed high-performance SCs for military applications[27,29], which found further applications as power sources for activators or RAM devices, telephones, *etc*[22,23]. Recently, other carbon materials like carbon nanotubes (CNTs) and graphene analogues have received enormous scientific attention[21–23].

3 Device Architecture

SCs belongs to a family of electrochemical capacitors and electric double-layer capacitor (EDLC) whose energy is stored by ionic species at the electrode/electrolyte interphase through charge transfer[14,15,19,21–23,27,30–32]. The stored energy depends on the available specific surface area of the electrode, the electrolyte ions' size, and the electrolyte's electrochemical potential stability window[14,21–23]. As shown schematically in Fig. 3, structurally, all SC

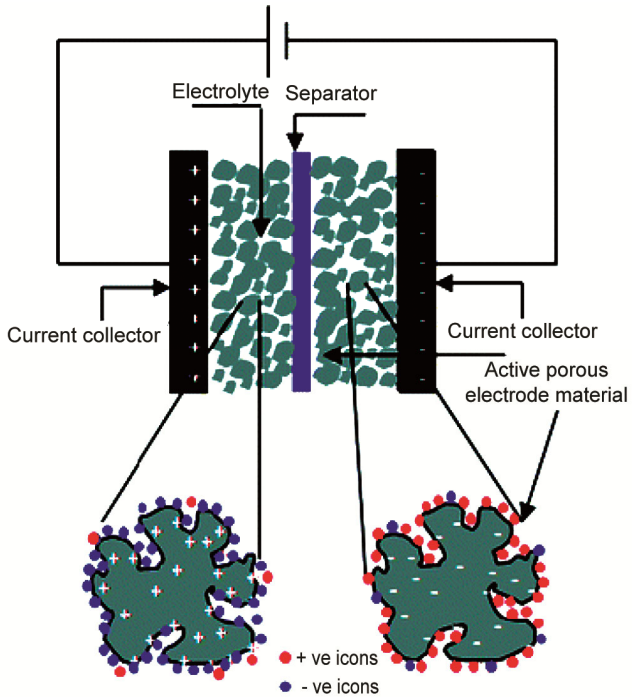

Fig. 3 — Schematic of EDLC displaying charge separation at electrode-electrolyte interface[22].

devices consist of two highly porous electrodes (*e.g.*, based on porous carbons or metal oxides), a polymeric electrodes separator, and an electrolytic medium[14,22,23]. The separator acts as a membrane that allows charged ions to be moved across and provides electrical isolation between closely packed electrodes. The electrolyte acts as an ion's source, enabling its movement from one electrode to another. The electrodes are in close contact with current collectors, which assures good interfacing between the electrodes and facilitates effective charge collection for external supply.

4 Types of Supercapacitors

SC devices can be broadly classified into two categories (Fig. 4) based on the charge storage mechanism and nature of active electrode materials[19,22,23]:

(i) Electrochemical double-layer supercapacitors (EDSC)
(ii) Electrochemical capacitors or Faradic or pseudocapacitors

The EDLC-type charge storage is the consequence of molecular distance level separation of charges at the electrode/electrolyte interface of highly porous electrode material[14,22]. Consequently, its charge storage capacity is governed by the accessible specific surface areas of electrode material. Carbon-based

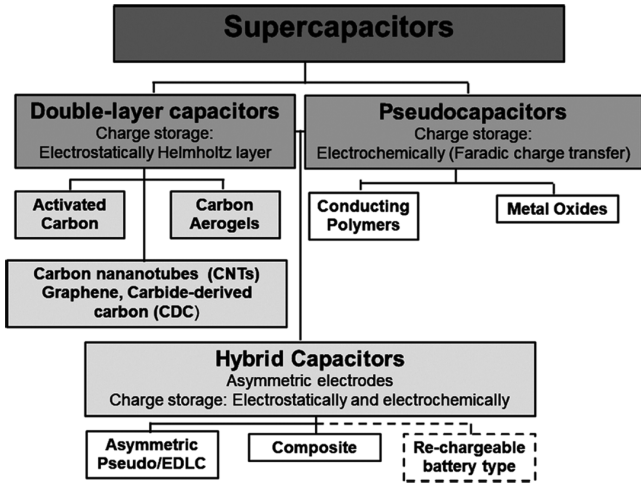

Fig. 4 — Classification of supercapacitors.

porous materials are the most common example of EDLC or electrolytic SCs. In contrast to EDLCs, the pseudocapacitive action depends on the fast faradic redox reactions[20,28]. Pseudocapacitors or electrochemical capacitors include metal oxides and conductive polymer-based materials[21,23,33], which undergo reversible redox reactions on the electrode's surface or inside bulk, producing storage action. The hybrid SCs combine the anode of EDLC SC with the cathode of the pseudocapacitor, resulting in both high specific capacitance and high energy density[22,23,33].

5 Electric Double-Layer Supercapacitors (EDLCs)

EDLCs are energy storage devices that store the electrical energy directly in the molecularly separated ionic double layer at the electrode/electrolyte interface[19–23,27,28,34–38]. At a metal/solution interface, a thin charge layer is formed on the metal surface due to excess/deficiency of electrons. In contrast, anionic layer of opposite charge is formed over the metal surface in contact with the electrolyte due to excess cations/anions. Therefore, an electrical double layer forms due to the dipolar assemblage of charges at the metal/electrolyte interface. As already discussed, EDLC has a pair of porous electrodes formed over current collectors and electrically isolated by an ion-transporting separator and flooded with an electrolyte medium[14,20]. It is essential to note that the electrodes are often made from nanomaterials with peculiar features of high porosity and surface area (500 – 2000 m^2/g). The charges are stored in the meso- and micro-pores at the interface between the electrode's surface (including pore walls) and suitable ionic electrolytes. In analogy with parallel plate capacitors, the charge storage capacity of EDLCs can be expressed as:

$$C_T = \varepsilon_o \varepsilon_r \frac{A}{d} \quad \text{... (1)}$$

where 'C_T' is the total capacitance of the electrode (in farads), 'ε_o' is the permittivity of vacuum, 'ε_r' is the dielectric constant of the electrolyte, 'A' is the surface area of the electrode available to electrolytic ions, 'd' is the effective thickness of the electrochemical double layer. Therefore, nanostructured electrode materials possessing high specific surface area and molecular thickness of the double layer (~few nanometers) are in-general responsible for the colossal capacitance of the supercapacitors. Besides, the wettability of the electrodes' surface by electrolyte affects the accessibility of pores, available surface area, and double-layer thickness. Generally, the specific capacitance of various carbon electrode materials in the organic electrolyte is much lower than that in aqueous electrolytes[21–23] due to the less accessibility of surface pores by the ions in organic electrolyte because of the bigger size of organic ions compared to available pore dimensions. Further, the aqueous electrolytes possess a higher dielectric constant than organic electrolytes, contributing to the high specific capacitance of the former. In addition, the electrolyte also affects the supercapacitor voltage, *e.g.*, the lower value for an aqueous electrolyte (~ 1.0 V)compared to the organic electrolyte (2.5–2.7 V) can be correlated with better electrochemical stability and wider potential window of the latter.The complete SC device can be visualized as two separate capacitors connected in series, *i.e.*, one formed by a positive electrode with capacity 'Cp' and the other by a negative electrode with capacitance 'Cn' such that the effective capacitance (C_T) of the device can be expressed as:

$$\frac{1}{C_T} = \frac{1}{C_p} + \frac{1}{C_n} \quad \text{...(2)}$$

If the two electrodes are identical (*i.e.*, Cp = Cn), the C_T value of such symmetric SC would be half of any electrode's capacitance, *i.e.*, C_T=Cp/2=Cn/2. In contrast, for asymmetric SC devices, where Cp≠Cn (*i.e.*, the anode and the cathode are constituted by different electrode materials), the CT value is governed by the electrode having a smaller capacitance value. Upon charging the SC, a voltage (V) will build up across the two electrodes, such that the stored energy(E) and output power (P) of the device can be expressed as[14,19,23]:

$$E = \frac{1}{2} C_T V^2 \text{ and } P = \frac{V^2}{4R_s} \quad ...(3)$$

where V is the cell's output voltage (in volts), and R_s is the device's equivalent series resistance (ESR). Generally, a highly effective SC should display a large C_T value, high operating potential (V), and a minimum R_s. The electrochemical potential window or thermodynamic stability of the electrolyte solution restricts the V. In contrast, R_s arises from the combined effect of electrode resistance, electrolyte solution resistance, mass transfer resistance of the ions, and contact resistance between the current collector and active electrode material[14,22,23].

There are primarily three methods for storage capacity determination of various electrode materials, viz. constant current charge/discharge (CCD), cyclic voltammetry (CV), and electrochemical impedance spectroscopy (EIS), as shown schematically in Fig. 5[14,19,33]. The first method estimates capacitance (C) assuming an ideal capacitor condition where the charge-discharge curve is linear so that capacitance (C) can be calculated from the ratio of current (I) and slope as C=I/slope (see Fig. 5(a)). The second method ignore any redox process so that the cyclic voltammogram is considered as rectangular (see Fig. 5(b)) with the capacitance value equal to the ratio of half the value of the saturation currents difference and potential sweep rate. In the EIs technique, the low-frequency components representing the capacitive region are identified in the impedance versus frequency plot (see Fig. 5(c)) to determine the capacitance using established mathematical expressions. In addition, modeling the data with equivalent circuits provides an alternative way of extracting capacitance value from the EIS data.

6 Models for Supercapacitors

The charge storage is governed by the arrangement of charged species at the metal/solution interface known as the "electrical double layer," which is formed at a particular potential. Typically, the aerial capacitance values are 10-40 mF/cm^2, which scales with the applied potential, contrary to ideal capacitors where capacity remains applied potential independent. In this regard, different models have been developed to explain the mechanism and response of electrodes under the given applied potential in solution[20,22,23,28,39–44].

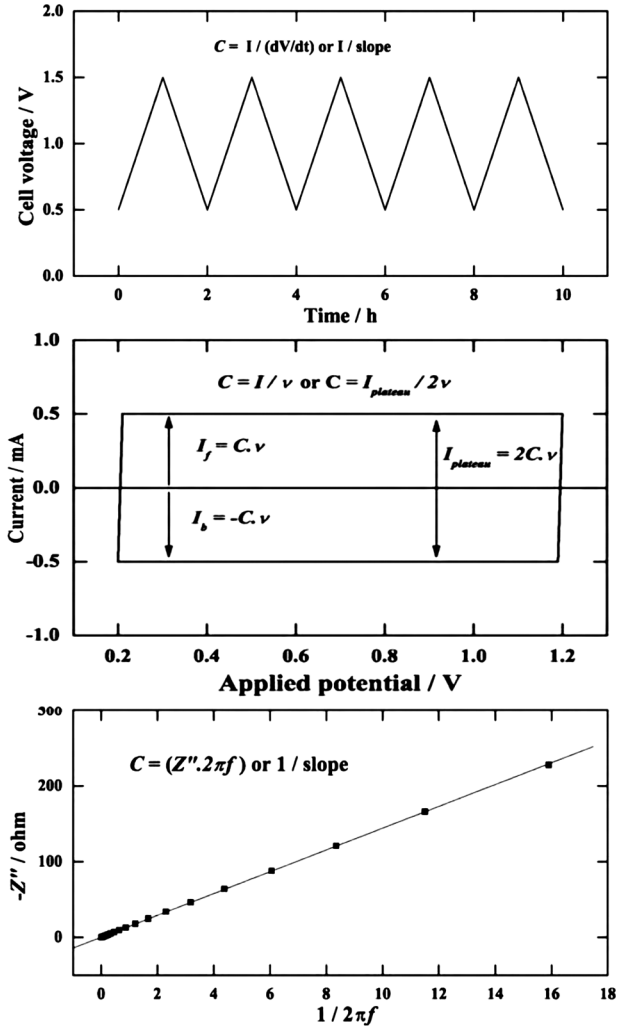

Fig. 5 — Idealised schematic representation showing measurement of capacitance of supercapacitor devices and electrodes from (a) constant-current charge–discharge curve; (b) cyclicvoltammogram(rectangular component of response, ignoring redox peaks); (c) low-frequency component of imaginary impedance data from electrochemical impedance spectroscopy (EIS); where C is capacitance (F), I is current (A), ν is scan rate (V/s), Z" is imaginary impedance (ohm), f is frequency (Hz), (Reprinted from[33] with permission from Elsevier).

6.1 Helmholtz Model

An interface is formed upon contact between the electrode material and solid/liquid electrolyte, which acts as the electrostatic charge storing resorvoir[40], as shown schematically in Fig. 6(a).

According to this model, the differential capacitance can be expressed as:

$$C_I = \frac{\varepsilon}{4\pi d} \quad ...(4)$$

where 'ε' is the relative permittivity of the electrolyte medium and 'd' is the average distance between

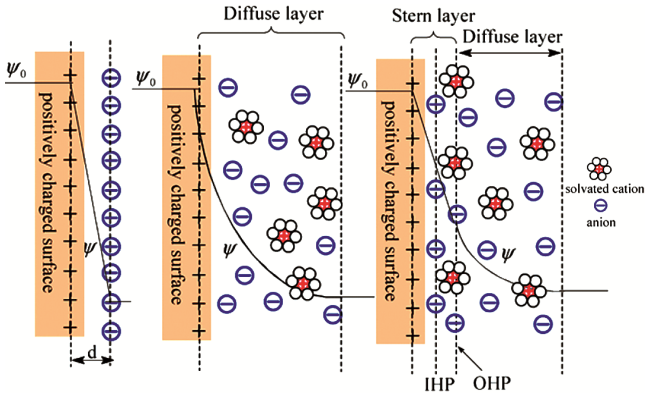

Fig. 6 — Models of the electrical double layer at a positively charged surface: (a) the Helmholtz model, (b) the Gouy–Chapman model, and (c) the Stern model, showing the inner Helmholtz plane (IHP) and outer Helmholtz plane (OHP.), (Reprinted from[23] with permission from RSC).

opposite charges stored at the electrode/electrolyte interface. This model revealed the linear dependence of the stored charge on the applied voltage. However, in this model, crucial factors were overlooked, such as adsorption onto the surface, the interaction between solvent & electrode and diffusion/mixing of ions in the electrolyte medium.

6.2 Gouy – Chapman Model

The independent observations by Gouy and Chapman in 1910 & 1913, respectively, pointed out that otherwise thought double layer capacitance scales with the ionic concentration of electrolyte and applied potential. In this model,[41,42] introduction of a diffuse model of the double-layer is made such that the metal's surface distance dependence of charge distribution of ions causes an exponential decrease of potential away from the fluid bulk surface, thus allowing the use of Maxwell–Boltzmann statistics. The proposition of Gouy accounts for this behavior: thermal motion kept the ions from accumulating on the surface of the electrode and forming a diffuse space charge (Fig. 6(b)). In this model, the ions were considered as point charges. The Boltzmann equation was used to determine the distribution of ions. In contrast, the Poisson equation was used to relate the charge density with potential, such that the differential capacitance can be expressed as:

$$C_G = \frac{\varepsilon\kappa}{4\pi}\cosh\frac{z}{2} \qquad \ldots(5)$$

where 'z' is the ion's valency whereas'κ' is the inverse Debye-Hückel length that can be further mathematically written as:

$$\kappa = \sqrt{\frac{8\pi n e^2 z^2}{\varepsilon kT}} \qquad \ldots(6)$$

where 'n' is the ion density or ions/cm^3, 'k' is the Boltzmann constant, and 'T' is the temperature in kelvin. Thus it is evident from equations (5) and (6) that the C_G is not a constant term.

6.3 Stern and Grahame Model

In 1924, Stern introduced a compact layer (comprising a layer of specifically adsorbed ions) in addition to a diffuse layer to further modify the Gouy-Chapman model[43,44]. In this model (Fig. 6(c)), the minimum distance between the diffuse ions and the surface of the electrode is referred to as the "Outer Helmholtz Plane (OHP)" (or Gouyplane). In contrast, the ion layer adsorbed over the electrode's surface is called the "Inner Helmholtz Plane(IHP)."The capacitance due to the Stern layer (C_1) was combined in series with that due to the diffuse layer (C_G) by the Grahame in so that effective capacitance (C) can be expressed as:

$$\frac{1}{C} = \frac{1}{C_1} = \frac{1}{C_G} \qquad \ldots(7)$$

In case of specific ionic adsorption, equation (7) becomes in applicable and capacitance can be mathematically represented in terms of differential of surface charge as:

$$\frac{1}{C} = \frac{1}{C_1} + \frac{1}{C_G}\left(1 + \frac{\partial\sigma_A}{\partial\sigma}\right) \qquad \ldots(8)$$

where'σ_A'is the surface charge of the adsorbed ions and 'σ' is charge density over electrode. The only drawback of this model is that it ignored possible capacitive effects resulting from interactions between dipoles and the charged electrode surface.

6.4 Bockris-Devanathan-Muller (BDM) Model

Bockris, Devanathan and Muller (BDM) proposed a further evolved model in 1963 to include solvent effects[45]. It is highlighted that a layer of solvent was also present at the changed electrode's surface, *i.e.*, within that, the field created by these charges led to the preferred alignment of the molecular dipoles of the medium. Therefore, it is evident that specifically adsorbed ions having fixed dipolar orientation would displace few of the electrolyte molecules. In contrast, the dipoles in the following layers (away from the charged electrode) would not be as fixed as those in

the first layer and assume relatively random orientation.

7 Pseudocapacitors

The second electrochemical supercapacitor type is pseudocapacitor (*e.g*., metal oxides like ruthenium oxide or electro-active molecules like conjugated polymers), wherein the energy storage mechanism is due to fast and reversible electrosorption or redox reactions, occurring on electrode's surface through various faradic or non-faradic processes[20,21,23,27,28,30,33,46]. In general, the pseudocapacitance phenomenon is attributed to three distinct types of charge transfer processes:

(i) surface adsorption of ions from the electrolyte
(ii) reversible redox (oxidation-reduction) reactions
(iii) reversible doping/undoping of electro-active conducting polymers.

The first two processes are very sensitive to the available specific surface area of the electrode. In contrast, the third is a bulk-related phenomenon with less dependence on the surface area, although it still requires porous channels for ionic transport. For example, the ruthenium oxide films in aqueous sulphuric acid medium display pseudocapacitance[23,46,47] where in reversible and fast electron transfer occurs followed by electro-adsorption of H^+-ions on the surface of ruthenium oxide particles as chemically represented below:

$$RuO_2 + xH^+ + xe^- \leftrightarrow RuO_{(2-x)}(OH)_x \quad ...(9)$$

The Nernst equation gives the potential E as:

$$E = E_0 + \frac{RT}{zF}\ln\frac{\Re}{1-\Re} \quad ...(10)$$

where E_0 is the standard reduction potential of electrode material, R is the universal gas constant, T is the temperature in Kelvin, F is Faraday constant, and $\Re$ is ratio ex pressed as [oxidant$_{conc.}$ / (Oxidant$_{conc.}$+ Reductant$_{conc.}$)], the amount of charge (nF) is a function of the potential (E). These capacitors are costly, and their high manufacturing cost limits large-scale production. Recently, several studies have been devoted to MnO_2 as a lowcost alternative to RuO_2.The main drawback of the oxide (RuO_2 or MnO_2) based pseudocapacitors is that they operate in combination with an aqueous electrolyte which constrains the operative cell voltage below 1.5 V. In actual practice, both EDLC and pseudocapacitor storage mechanisms co-exist in supercapacitor systems, though in most cases, one of the storage mechanisms dominates (*i.e*.,>95% contribution) over the other.

8 Hybrid Supercapacitors

Hybrid supercapacitors tend to bridge the gap and combine the specific advantages of EDLCs and Pseudocapacitors to realize superior performance[19,20,23,48]. Here, fast and reversible Faradic reactions and parallel non-Faradic processes work together for charging/discharging events. This enabled the achievement of better energy and power densities than EDLCs with superior cycling stability and lower cost than pseudocapacitors. Technically three different types of hybrid super capacitors can be identified, differing in terms of electrode configuration, viz. composite (where in one or both electrodes are made up of mixed-phase or composite materials), asymmetric (wherein both electrodes are of different materials); and battery-type (capattery or battery-capacitor combination), which are beyond the scope of this article. It is clear from the previous discussions that designing of efficient and improved supercapacitor needs a large capacitance (C_T) value, high voltage window (V), and low equivalent series resistance (ESR or R_s)[14,23]. The value of C_T depends upon the electrode material, its specific surface area, surface functionality, wettability characteristics, porosity, pore size, and size distribution whereas the electrochemical stability potential window of the electrolyte medium decides V. The R_s receive the contributions from the contact resistance between the current collector and electrode, the electrode's ohmic resistance, the mass transfer resistance of the ions in a given electrolyte medium, and the ohmic resistance of the electrolyte solution. Therefore, electrode material and electrolytes are important and discussed in the next section.

9 Electrode Materials

A diverse variety of electrode materials can be selected for supercapacitors depending upon the preferred storage mechanism, *e.g*., double-layer capacitance, pseudo capacitance, or their combination. These materials can be broadly classified into three main categories[21,23,30,33,46,49,50]:

(i) carbon-based materials (micron-/nano-sized materials): they are mainly EDLC type
(ii) transition metal-based materials: they are pseudocapacitive
(iii) conducting polymer-based materials: they are pseudocapacitive

Some of the commonly used electrode materials, electrolytes used, working voltage, and specific capacitance values are listed in Table 2[50].

9.1 Carbon-based materials

Carbon-based materials are obtained by thermal carbonization of suitable carbon precursors like coal/pitch, biomass (*e.g.*, wood, straw/stubbles, coconut shells, rice husk, etc.), or polymers (*e.g.*, polyacrylonitrile or even thermosets/thermoplastics) followed by post-treatment. The hot gases (*e.g.*, nitrogen, hydrogen, carbon dioxide, or steam flux) are used for post-treatments resulting in high specific surface area and open pore structure. Carbon-based materials like. carbon aerogels, graphites, CNTs, carbon nanofibers, and nano-sized carbons (Table 3) are known to display stable yet with high capacitance with EDLC as the predominant charge storage mechanism due to inherent high electrical conductivity, large specific surface area, controlled porosity with good pore accessibility, high chemical & electrochemical stability, high thermal stability[19,21,23,34,36,48–50].

Table 2 — Different electrode materials for supercapacitors[50].

Material	Electrolyte	Working Voltage (V)	Specific Capacitance (F/g)
	Carbon based materials		
Activated carbon	1M Et_4NBF_4 + PC	1.5	40
Carbon nanofibers	1 M KOH	1.0	192
Graphite	1M Et_4NBF_4 + PC	3.0	12
Carbon aerogels	1.5M Et_3MeNBF_4 + PC	3.0	160
AC fibre cloth	6M/L KOH	1.0	208
SWCNTs	EMITFSI	2.3	50
MWCNTs	1.96M $TEMABF_4$ +PC	2.5	13
Mesoporous carbon	30 wt% KOH	0.9	180
Few layered graphene	1 M H_2SO_4	0.8	186
Graphdiyne	Na_2SO_4	1.0	71
	Conducting Polymers		
PANI	Gel polymer electrolyte	0.7	259
PPY	PVDF-HFD gel electrolyte	0.8	78-137
PTh	1 M H_2SO_4	1.2	72
PANI/RGO	1 M H_2SO_4	0.8	241
PANI/MnO_2	0.1 M Na_2SO_4	1.2	715
PANI	Gel polymer electrolyte	0.7	259
PANI/activated carbon	6 M KOH	0.9	588
	Transition Metal Oxides		
$RuO_2.H_2O$	0.5M H2SO4	1.0	650
MnO_2	0.5M K2SO4	0.8	261
$Ni(OH)_2$	3% KOH	0.8	578
$MnFe_2O_4$	1M $LiPF_6$ + EC/EMC	2.5	126
TiN	1 M KOH	0.2	238
V_2O_5	2 M KCl	0.7	262
WC/carbon	1 M H_2SO_4	0.9	477
Co-Ni oxides/CNTs	1 M KOH	1.0	569

Table 3 — Different carbon materials and structures used in EDLCs[51].

Material	Carbon onions	Carbon nanotubes	Graphene	Activated carbon	Carbide derived carbon	Templated carbon
Dimensionality	0D	1D	2D	3D	3D	3D
Conductivity	High	High	High	Low	Moderate	Low
Volumetric capacitance	Low	Low	Moderate	High	High	Low
Cost	High	High	Moderate	Low	Moderate	High
Structure	Onion-like concentric spherical shells	Concentric cylinders	2D sheet	3D porous graphitic framework	3D porous graphitic framework	3D porous graphitic cage-like framework

9.1.1 Activated Carbons

Activated carbons (ACs) are widely used active electrode materials with EDLC-type charge storage mechanisms due to merits such as high specific surface area (SSA), high porosity, good electrical conductivity, good chemical/electrochemical stability, high thermal stability, corrosion resistance, facile synthesis from a variety of cheap precursor available in plenty[48]. ACs are generally prepared from carbon-rich organic precursors via carbonization and physical or chemical activation to obtain the high SSA and controlled porosity (pore size, volume, and size distribution)[36]. Physical activation involves heat treatment in the temperature range of 700-1200 °C in the presence of oxidizing gasses (*e.g.*, air, steam, or carbon dioxide). In contrast, the chemical activation is carried out at relatively lower temperatures (400-700 °C) and using chemical activating agents (*e.g.*, NaOH, KOH, H_3PO_4, or $ZnCl_2$)[52–54]. Literature shows that based on carbon precursor and adopted activation route, ACs with very high SSA(*e.g.*, upto 3000 m^2/g, which is even greater than graphene!) can be prepared with varying structural, electrical and electrochemical properties attributes[36,38,52–56]. The activation process produces a porous frame work within the carbon material's bulk such that three size range pores can be identified, viz. micropores (< 2 nm), mesopores (2< and <50 nm), and macropores (> 50 nm) as shown schematically in Fig. 7.

As already discussed, carbon-based materials' theoretical specific capacitance (*i.e.* capacitance per unit weight usually expressed in the unit farad per gram, *i.e.*, F/g) is proportional to their SSA. However, the large solvated ions (particularly in organic solutions compared to aqueous medium) are relatively more difficult to absorb by micropores than mesopores. As a result, only a fraction of available SSA is accessible for charge storage leading to reduced capacitance, problems in maintaining a high charge-discharge rate, and low energy/power density. Due to the above reason,the measured capacitance of a given ACs in the same device is often higher in aqueous electrolytes than in organic electrolytes [36,51,55–57]. Recent studies have provided conclusive evidence that maximum EDLC performance is achieved upon pore size matching between electrode pores material and counter-ions size of electrolyte[21,51],*e.g.*, carbide-derived-carbons (CDCs) electrode-based EDLC display maximum capacitance (Fig. 8) for ~0.7 nm pore size which is near the larger dimension of the counter-ions of ionic liquid EMI–TFSI.

The surface chemistry (*e.g.*, type, nature, and concentration of functional groups) of AC is another critical parameter that can affect specific capacitance, rate capability, and device stability under continued cycling. It was found that oxygen functionality-rich ACs in the presence of aqueous electrolytes give high energy/power density, good capacity retention, and fast charging-discharging ability[58,59]. However, employment of these surface functionalized AC in commercial supercapacitors, which operate at high potentials and in the presence of organic electrolytes, leads to electrodes' mechanical, electrical, and electrochemical instability and may even trigger the electrolyte decomposition. Therefore, it is crucial to maintain the optimum balance between surface area, porosity, and chemical nature of the electrode's

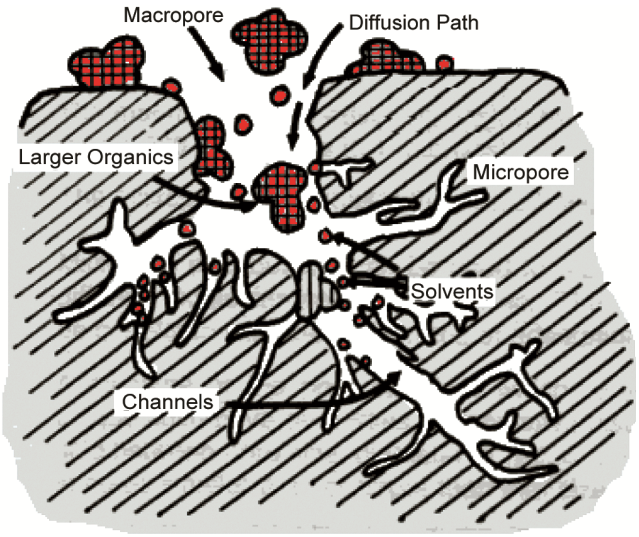

Fig. 7 — Schematic representation of different types of pores in Activated carbon.

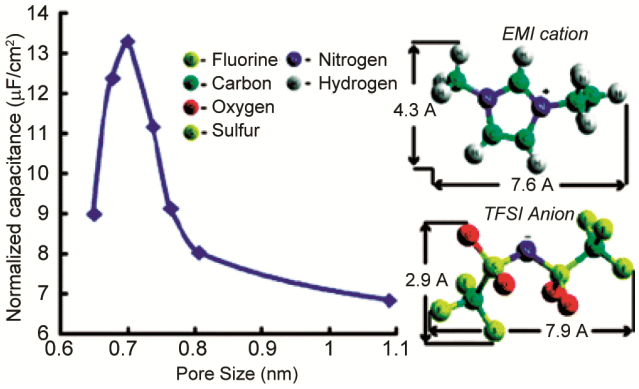

Fig. 8 — Variation of capacitance as a function of pore size for CDC samples in the presence of Ionic liquid (EMI–TFSI) based electrolyte (Reprinted from[51] with permission from ACS).

surface, to realize stable, high storage capacity and rapid power deliverability of electrode materials. In a nutshell, it can be said that despite high SSA, the regulation of pore size, shape, and distribution of ACs and control of their surface functionalities and wetting characteristics, are still challenging issues. Therefore, coherent strategies are required to prepare tailored ACs possessing controlled porosity, electrical properties, and surface chemistry to realize advanced supercapacitors with enhanced energy/power density, fast charge/discharge capability, and good stability under continued cycling (charge/discharge).

9.1.2 Activated Carbon Fibers (ACFs)

ACFs are important electrode materials of EDLCs due to their high aspect ratio, large specific surface area, high electrical conductivity, and chemical/electrochemical stability. Unlike carbon powders requiring binders, they can be directly used as active material in the form of freestanding films, thus eliminating the contact resistance between particles and conductivity reduction due to binder. ACFs can be synthesized from polymeric fibrous precursors such as rayon or poly-acrylonitrile by controlled heat treatment under a regulated atmosphere. ACFs offer several advantages over conventional powdered activated carbons[60–63], *e.g.*, high specific surface area & pore volume, narrow pore size distribution, high ions adsorption/desorption rates, mechanical strength, flexibility, thermal, chemical & electrochemical stability and ability to be integrated into the form of textiles that makes them a promising candidate for flexible, robust and efficient supercapacitors. ACFs can be obtained from polymeric fibrous precursors(*e.g.*, Rayon, Polyacrylonitrile, Nomex) either by physical activation [*e.g.*, controlled carbonization followed by gasification, or direct heating in the atmosphere of oxidizing gases like steam or carbon dioxide or both] or chemical activation [treatment with a chemical activating agent like as $ZnCl_2$, H_3PO_4, KOH/NaOH followed by pyrolysis]. Subsequently, the AC is thoroughly washed to remove the residual activating agent and other impurities. Once activation is complete, the specific surface area is often comparable to ACs with mesoporous range pores ideal for the sorption of electrolytes. The surface area of AFC-based textiles is very high, and based electrodes display low electrical resistance along the axial direction and low contact resistance to the current collector[47,60,63]. The AFC-based electrodes exhibit predominantly EDLC response (due to easily accessible micropores) with only minor pseudocapacitance (due to specific surface functional groups).

9.1.3 Carbon Nanotubes (CNTs)

Over the last few years, CNTs have drawn enormous attention due to fascinating properties like good mechanical strength, high electric conductivity, excellent chemical/thermal stability, good electrolyte accessibility, tuneable surface chemistry, and a wealth of prevalent applications[64–66]. Multi-walled CNTs (MWNTs) and single-walled CNTs (SWNTs, Fig. 9) have been exploited as supercapacitor electrode material[34,67–72].

Niu *et al.*[70] first demonstrated using CNTs as active electrode material for supercapacitors. The high mechanical strength, structural flexibility/resilience, highly wettable surface for non-polar electrolytes, and outstanding electrical/thermal conductivity of CNTs, often result in high rate charging-discharge capability, high power density, and relatively better capacity retention during repeated electrochemical cycling[67,73]. It is essential to point out that, despite their low SSA, higher capacitance values were measured for CNTs (for both MWNTs and SWNTs)[34,67,70], compared to ACs, mainly due to the dominant mesoporosity of the CNTs (in contrast to ACs that contains mainly micropores which are difficult to be accessed by the

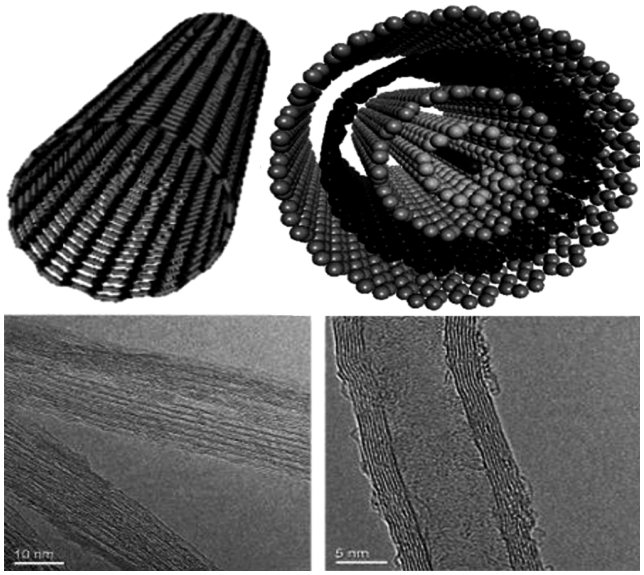

Fig. 9 — Schematic representation of single wall carbon nanotubes (SWCNTs, Top-left) and multi wall carbon nanotubes (MWCNTs, Top-right) alongwith their TEM images showing SWCNT bundles (Botton-left) and individual MWCNT (Bottom-right), (Reprinted with the permission).

solvated counter-ions) contributed by the entangled tubular networks that make CNTs' surface highly accessible to the electrolyte (*i.e*., improves accessible surface area) and lead to high specific capacitance. The excellent electrical transport properties of CNTs facilitate rapid charge injection/withdrawal and contribute towards high capacitance even at high frequencies that directly conveys the better power performance (*i.e*. fast energy deliverability) required for techno-commercial applications. Recently, it has been demonstrated that aligned CNTs are more efficient in promoting ionic transport compared to the entangled CNTs, due to the irregular and thus difficult to be accessed pores in the randomly entangled system[69]. Therefore, several efforts have been made to use aligned CNTs to derive an advantage in high power density[74]. The energy density value ~ 36 Wh $kg^{-1}$and superior rate capability than ACs-based system is obtained. It has been highlighted that the chemical activation process can realize the specific energy of CNTs to enhance their SSA and pore volume[47]. The specific capacitance can also be enhanced by suitable modification of CNT's surface, leading to improved wettability and induction of pseudo-capacitance. For example, pristine CNT having inherent hydrophobicity display low specific capacitance, whereas surface-functionalized CNTs display several times more BET SSA, pore volume and specific capacitance than former. However, like other high SSA activated carbon surfaces, the cycling life tends to be limited after the activation. Therefore, optimumization between the porosity and conductivity is required to realize high capacitance as well as power density or rate capability. Nevertheless, despite their excellent electrical and mechanical properties, poor surface properties, limited SSA and high cost of production/purification of CNTs limited their use for high specific storage capacity EDLCs and dedicated R&D efforts are required to eliminate the above-mentioned drawbacks.

9.1.4 Templated Porous Carbons (TPCs)

TPCs are nanostructured carbons with ordered pore morphology, controlled porosity (*i.e.*, pore size, volume, and size distributions), interconnected porous networks, and tailored surface chemistry leading to high SSA, low resistance (due to reduced tortuosity of ion-diffusion path) and fast charge-discharge capacity (due to rapid sorption-desorption of ions)[75–77]. TPCs are formed by the controlled impregnation of the pores of the specific template (silica sphere, SBA-15 or Zeolite-Y) with suitable carbon precursor, subsequent carbonization process, and finally removal of the template by chemical etching, ultimately leaving behind a porous carbon framework as shown schematically in Fig. 10. It's a promising route to realize ordered nanoporous carbons having regulated conductivity, porosity, and physicomechanical properties through judicious selection of the template, carbon precursor and carbonization temperature. Ryoo *et al*. first prepared ordered mesoporous carbons (OMCs) having controlled pore diameter and high pore volume[78,79] exploiting the hard template nanocasting strategy. Later OMCs were demonstrated for their excellent electrochemical performance and superior response as electrode material for EDLCs compared to other carbon analogues. It has been shown that mesopores (2-5 nm) can improve the rate capability/power-density through facile shuttling of counter-ions in the electrode's pores.

In contrast, the accessible micropores (<2 nm) contribute to high energy-desnity[80,80,81]. Again, the

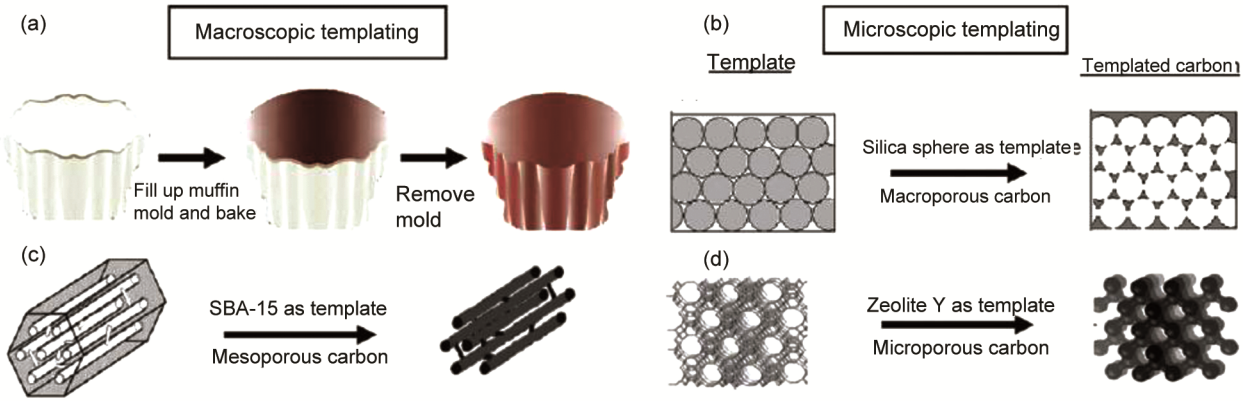

Fig. 10 — (a) Schematic of cacroscopic templating; microscopic synthesis of (b)macroporous carbons using silica spheres as template, (c) mesoporous carbons using SBA-15 as template and (d) microporous carbons using zeolite Y as template, (Reproduced from[22] with permission from RSC).

agreement between pore dimensions and ion size influences energy storage and power delivery performance. For example, existing research demonstrated that the 2-5 nm pore size range is much greater than the size of solvated counter-ions and best suited for realizing improved energy- and power-densities.

Over the years, various carbon structures with regulated porosity have been produced from various template/carbon-precursor combinations and demonstrated for supercapacitors[81–84]. TPCs, with narrow pore size distribution and easily accessible pores (due to much greater size than electrolyte ions and ordered pore channels), give much better rate capability and energy density than ACs, which contain disordered pores having broad size distribution. Additionally, in TPCs, ordered porous structure and better accessibility of nitrogen- and oxygen-based surface functionalities extended significant contribution via pseudo-capacitance components, *e.g.*, zeolite Y template-based functionalized OMC display high gravimetric specific capacitance in aqueous electrolyte with good cyclability (>10000 cycles)[83]. Similarly,3-dimensional hierarchical porous graphitic carbons (HPGCs) with the structural architecture of macro-porous cores, meso-porous walls, and micro-porous channels have been demonstrated for high-rate capacity supercapacitors[82]. In such systems, the unique combination of various pores enhances energy and power density. The macropores serve as ion-buffering reservoirs, graphitic mesopore walls provide a high electrical conductivity framework, and micropores act as charge storage sites. So, charge storage and charge shuttling limitations are sorted out. The actual TEM/HRTEM images, a schematic of the 3D architecture, and the Ragone plots of the supercapacitors based on various carbon materials are shown in Fig. 11.

A colloidal-crystal templating technique[85] has also been demonstrated for regulated porosity ordered-porous-carbons possessing large specific surface areas and capacitance in combination with acidic electrolytes. It is evident from studies that micropores connected through meso- or macro-porous channels are charge storage reservoirs resulting in high specific capacitance, whereas the fast shuttling of electrolytes between interconnected channels contributes toward high power density and rate capability. Overall, the template route has emerged as one of the most

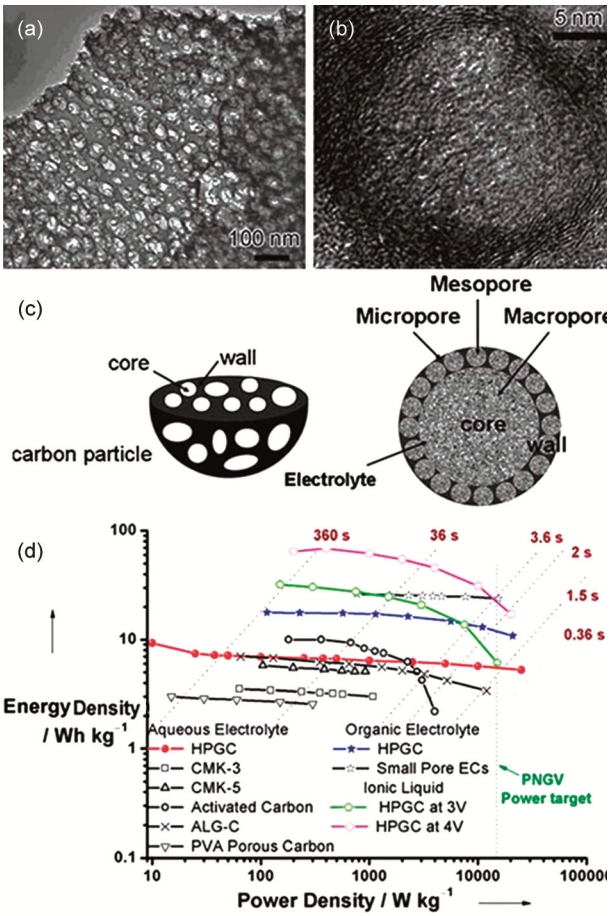

Fig. 11 — (a) SEM and (b) TEM images of HPGC, (c) schematic representation of the 3D hierarchical porous structure and (d) Ragone plot comparing the performance of HPGC compared to other types of carbons viz. CMK-3, CMK-5, activated carbon (Maxsob, Japan), ALG-C, PVA porous carbon, and small-pore EC. The dotted lines show the current drain time (© Wiley InterScience, reprinted with permission[82]).

promising solutions for designing ordered nanoporous solids[78,79] that regulate desirable physical and chemical attributes via a reasonable selection of the templates, carbon precursors, and carbonization conditions. They are also model materials for fundamental studies to extract vital information on the effect of pore size, shape, channel architecture, and electrical properties on the charge storage mechanism and its shuttling within interconnected porous networks.

9.1.5 Carbon Aerogels (CAGs)

The CAGs (or "frozen smoke") possess a monolithic 3D interconnected porous frame work containing high electrical conductivity carbon nanomaterials, forming controllable pore structures and relatively high specific surface area. CAGs can be

synthesized via a sol-gel route with subsequent pyrolysis organic precursor (*e.g.*, resorcinol-formaldehyde or phenol-furfural resinous gel), which removes the trapped liquid component of the gel[19,86,87]. Due to their very low density, high porosity, and good electrical conductivity, CAGs are an important alternate for supercapacitor electrode material, facilitating the realization of high energy and power density values. They enable thinner, lighter, more robust, and self-standing electrodes with high porosity and no requirement for a separate current collector. However, the dominance of mesopores is responsible for their low capacitance, which a suitable activation process can enhance for generating additional microporosity and resulting in the enhancement of accessible SSA. For example, it has been demonstrated that an as-prepared CAG sample displays a specific capacitance of ~80 F/g. KOH activation (treatment 900 °C for 2h) shows an increased specific capacitance value of ~145 F/g. It has been found that though there was a significant increase in BET surface area from 592 to 2371 m^2/g upon thermal activation, the capacitance increase was relatively low.[88]. The inaccessibility of the activation generated micropores and high internal resistance of the CAG framework result in a specific capacitance of ~104 F/cm^3 with an energy density of ~90 Wh/kg and power density of ~20 W/g[89].

9.1.6 Graphenes

Graphene is anatomically thin layer of hexagonally arranged carbon atoms, identified as the building block of all carbon materials, including graphite[19,90,91]. Due to its atomic thickness, graphene has an ultra high SSA of ~2630 m^2/g and ultimate charge storage capacity of 21 $mF/cm^{2,}$ which puts a theoretical upper limit of 550 F/g on the capacitance of all carbon materials[19,92,93]. Ruoff and coworkers reported the earliest work on graphene-based supercapacitors, who have synthesized chemically modified graphene for use as supercapacitors (Fig. 12(a))[93]. Despite partial agglomeration of graphene sheets, high SSA(>700 m^2/g) and specific capacitance (135 F/g)were realized in an aqueous electrolyte-based device. Due to the ultrahigh electrical conductivity of graphene, it can be directly exploited as supercapacitor electrodes (acting as an electrode and current collectors) for designing portable electronic complaint ultra-thin supercapacitor devices[95]. Recently, highly efficient supercapacitors have been assembled using curved graphene sheets (Fig. 13) to eliminate the face-to-face stacking tendency of layers. These sheets are assembled to form easily accessible mesopores readily wettable by ionic-liquid lectrolytes[92]. Such a powerful combination of electrode and electrolyte facilitates enhanced charge storage capacity, rapid sorption-desorption of ions, high operating potential (upto 4 V), and good device stability under cyclic operation (Fig. 14). This makes it possible to realize supercapacitor with energy density value of ~85 Wh/kg, which is near the Ni-metal hydride battery's storage capacity but possesses100-1000 times faster charging. The 2D architecture improves charging and discharging in graphene systems, especially carriers in vertically oriented sheets rapidly shuttle between deep inside of electrodes speeding up charging/discharging processes, making them even suitable for 100/120 Hz filter applications[96].

Ruoff group reported graphene-based SCs exploiting chemically modified graphene-based electrodes (Fig. 12(a)).[93] Despite the partial agglomeration due to the overlap of graphene layers, SSA up to ~700 m2/g and a high specific capacitance value of 135 F/g is achieved. Later, Rao and coworkers[97]exploited thermally exfoliated (1050 °C) reduced graphene-based electrodes for the device to

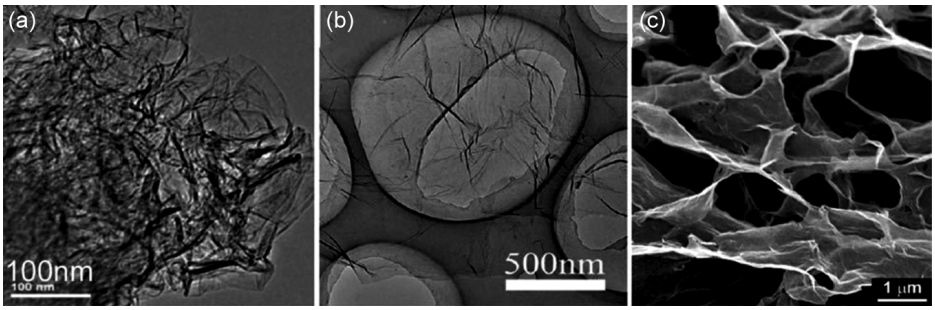

Fig. 12 — (a) TEM image of chemically modified graphene-based nanosheets, reprinted from [93] with permission, (b) TEM image of graphene nanosheets by a thermal reduction method, reprinted from [94] with permission, and (c) SEM image of a self-assembled graphene hydrogel, (Reprinted from [95] with permission).

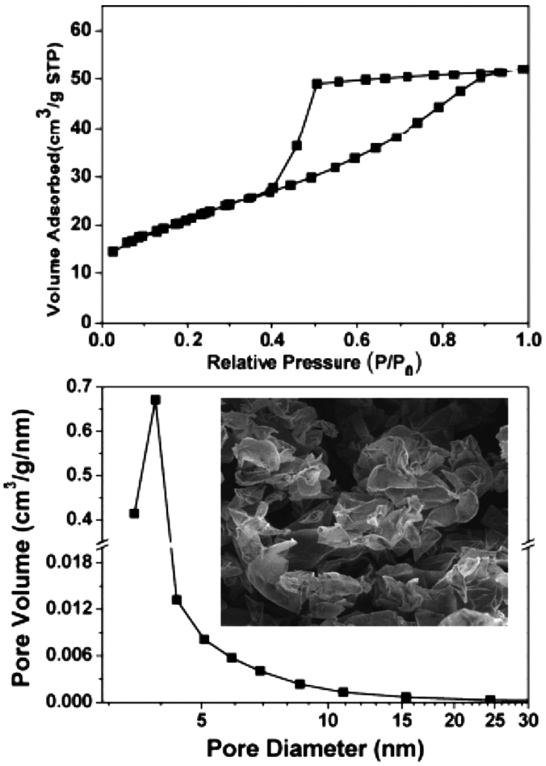

Fig 13 — Nitrogen adsorption isotherm (left image) and pore size distribution of the mesoporous graphene material (right image). Inset shows the SEM image of curve graphene sheets, (Reprinted from [92] with permission fom ACS).

demonstrate an SSA value of~925 m^2/g and a specific capacitance value of ~117 F/g. However, thermally assisted exfoliation is energy-intensive, costly, and complex to regulate. Yang and coworkers[94] worked in the direction of establishing a relatively low temperature (around 200 °C) exfoliation cum reduction route (Fig. 12(b)). The system displayed aggregated structure with large pores due to partial overlap between graphene nanosheets ultimately resulting in a specific capacitance value of 264 F/g. Because chemical or thermal reduction mediated graphene analogues have insufficient prores to access by electrolyte counter ions, porous graphene-based materials are easily necessary for achieving high energy density EDLCs[94,96,98]. Shi and coworkers[95] have demonstrated self-assembled graphene hydrogel having 3D porous architecture (Fig. 12(c)), possessing a high specific capacitance Value of 240 F/g at a current density of 1.2 A/g and in an aqueous acidic electrolyte medium. Other researchers have also highlighted that incorporating stabilizers/spacers between graphene layers improves SSA and hence specific capacitance and energy density[96,99–101].

9.2 Redox Pseudo-Capacitive Materials

In such types of capacitors, the energy is stored through redox reactions (faradic reactions), which are

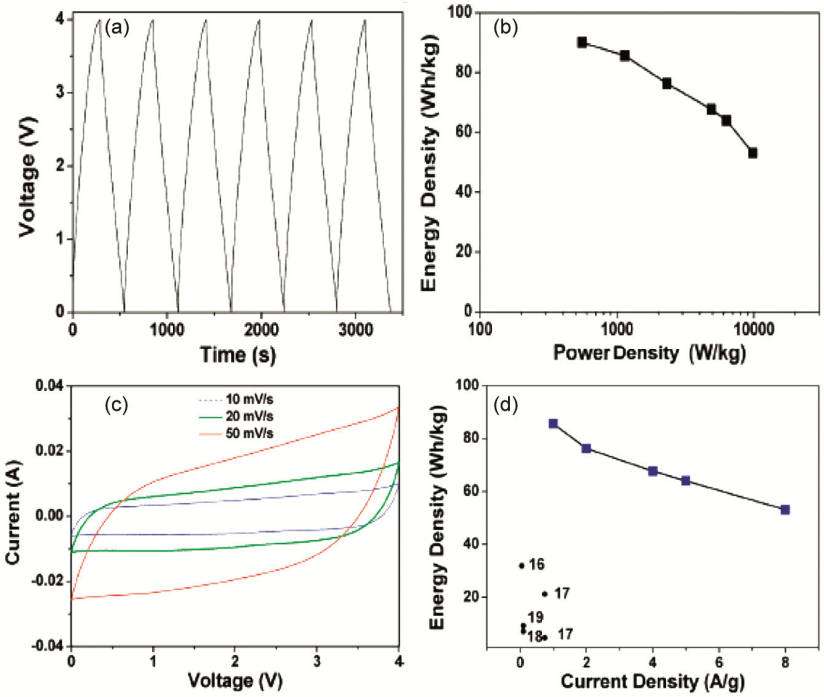

Fig. 14 — (a) Galvanostatic charge-discharge curve of a curved graphene electrode (6.6 mg each) at a constant current density of 1 A/g, using EMIMBF4 ionic liquid electrolyte; (b) Ragone plot of graphene supercapacitor, (c) cyclic voltammograms for graphene electrode at different scan rates using EMIMBF4 ionic liquid electrolyte; (d) relationship between the energy density and current density of a curved graphene electrode in EMIMBF4 ionic liquid electrolyte[92].

fast as well as reversible. The accepted or released electrons traverse across the double layer, constituting a similar process as during the charging/discharging of batteries[13,19,20,22,23,28,33,48]. The pseudocapacitive electron transfer occurs through various methods, viz. redox reactions involving preferentially adsorbed counter-ions from the electrolyte; electrosorption or intercalation of atoms in the layered structure; under potential deposition of hydrogen/metal atoms leading to faradaic charge transfer. These faradaic processes increase the specific capacitance as well as working voltage, ultimately resulting in the enhancement of both energy and power density as compared to EDLCs.

It is important to point out that the pseudo-capacitive materials not only store charges in the pores via the formation of a double layer (Fig. 15(a)) like EDLC but also undergo surface redox reactions within the bulk of the material (Fig. 15 (b)). Consequently, specific pseudo-capacitance values often exceed (10-100 times) carbon-based materials' capacitance (typically 10-25 μF/cm^2), again due to the involvement of surface as well as bulk in storing the charges. In general, pseudo-capacitive materials can be classified into two broad classes: conducting polymers and transition metal oxides[14,23,102]. However, metal nitrides have recently been reported as efficient pseudo-active materials.

9.2.1 Conjugated Polymers

Conjugated polymers (CPs) have been exploited as redox pseudocapacitor electrode materials due to high electrical conductivity (in doped state), ability to undergo fast and reversible oxidation/reduction processes, wide potential window, high porosity, tunable redox-activity via chemical alterations and large storage capacitycoupled with relatively low cost[33,34,48,102–108]. The repeat unit structures of the most commonly used CPs are shown in Fig. 16

Two types of charging processes can be identified, viz. p-doping with anions (oxidation) and n-doping with cations (reduction), as shown schematically below:

$$CP \rightarrow CP^{n+}(A^-)_n + ne^- \ (p-doping)$$
$$CP + ne^- \rightarrow (C^+)_n CP^{n-} \ (n-doping)$$

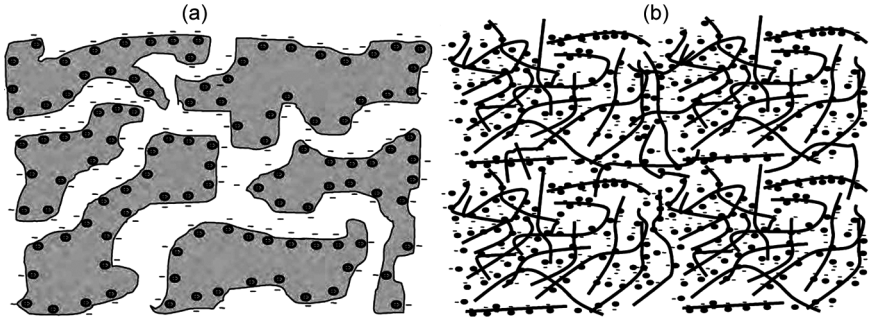

Fig. 15 — Comparison of charging of (a) double-layer capacitor (carbon) and (b) pseudo-capacitor, (Reprinted from[33] with permission from Elsevier).

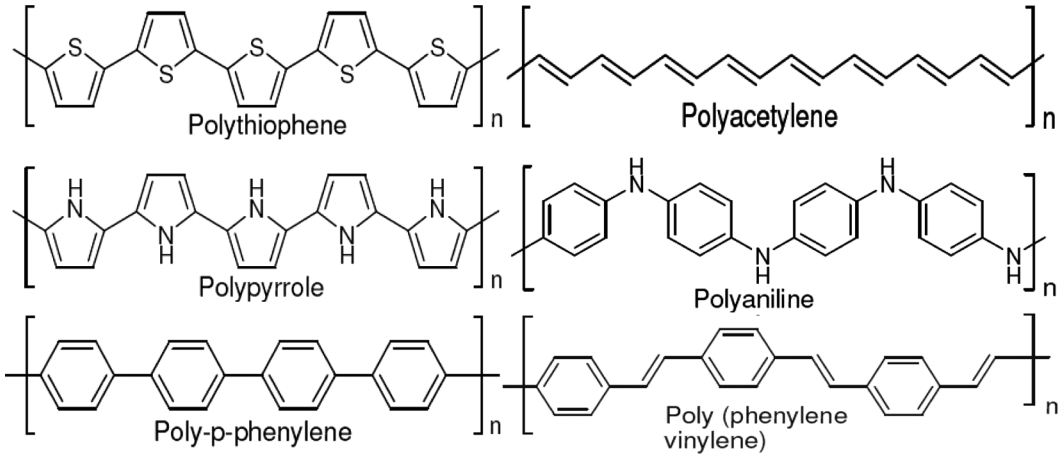

Fig. 16 — Chemical structures of some undoped conjugated polymers[102].

The forward and reverse reactions constitute the charging and discharging steps, respectively. The above charging/discharging process cause the physical expansion/contraction of the electrode (*i.e.*, swelling/deswelling) caused by the intercalation/ deintercalation of counter-ions during the doping/de-doping process[23,33,106]. Such rapid volume changes or swelling imposes mechanical stresses and may cause electrode failure due to fatigue loading under prolonged cycling. Consequently, the CPs-based pseudo-capacitors gradually degrade and show significant capacity reduction even for<1000 cycles. In contrast, the double-layer supercapacitors display excellent cyclic stability (upto 1,00,000 cycles). Therefore, though the pseudocapacitor's specific energy may be enhanced by increasing the degree of doping of electrode material, its often at the expense of stability due to counter-ions insertion/removal triggered mechanical stresses and triggered failure)[106].

Further, the ability of the electrode to undergo p- or n-doping, stability of doped forms, and operating potential window exerts a governing role in deciding the achieved specific energy and device stability. Polyacetylene and polythiophene (and its analogues) can be both p- and n-dopable. However, polyacetylene and poly-p-phenylene display high impedances (with low capacitance) upon n-doping, making them unsuitable as-ive electrodes. Similarly, polyaniline and polythiophene can only be p-doped (suitable as a cathode) due to the high-ive potentials required for n-doping, which often exceeds the electrochemical stability limit of the electrolytes. It has been found that n-doped polymers are more susceptible to electrochemical degradation than p-doped polymers and, thus, are more promising as electrode materials. Conducting polymers-based pseudocapacitors can have three configurations[107–111] with brief details as below:

(i) Type I (Symmetric or p-p configuration) is the same material p-dopable CP for both electrodes. Under charged conditions, one of the electrodes is in a fully doped state (p-doped). In contrast, the counter-electrode is present in its undoped/neutral form. The typical potential window for such a system is 0.75-1.0 V.
(ii) Type II (Asymmetric or p-p configuration) uses two different p-dopable polymers (*e.g.*, polypyrrole and polythiophene) for anode and cathode.
(iii) Type III (Symmetric or n-p configuration) employs the same polymer for both electrodes (*e.g.*, substituted polythiophenes) such that the p-doped form serves as the cathode (positive electrode), where as the n-doped form act as the anode (negative electrode). Their electrochemical potential window may extend upto 3V in a non-aqueous system.

A Type III device is the most attractive due to the high conductivity of the charged state as both electrodes are present in their highly conducting doped forms[108]. Moreover, the stored charge is released at higher potentials (upto 3V) compared to Type I and Type II devices[106,108], which is expected to contribute towards high energy and power density[33]. However, due to the practical difficulties associated with performing n-doping and relatively poor stability of n-doped forms, these devices are unsuccessful. Consequently, hybrid-type asymmetric devices may also be assembled[33,106,109] by combining CPs based positive and carbon-based negative electrodes.

It's worth mentioning that the usage of CPs-based electrodes critically depends on the polymer's electrochemical stability and electrolyte (Table 4). The permissible potential range (*i.e.*, max positive or negative potential value) within which the CP supercapacitor can work (i.e., electrochemical potential window) is strictly defined for a given CP/electrolyte system. Beyond this strict window, capacity deteriorates due to irreversible structural changes or the onset of a passive state, *e.g.*, at more positive potentials, the CP tends to degrade. In contrast, it may switch to an electrically insulating un-doped state at too negative potential values.

Polyaniline is an important CP that has been extensively explored as a candidate for supercapacitor

Table 4 — Various conducting polymers, their working voltge, specific capacitance and achieved performance as pseudocapacitor electrode material.

Conducting polymer for electrode material	Doping ability (p or n type)	Working Voltage (V)	Theoretical Specific Capacitance (F/g)	Measured Specific Capacitance (F/g)	Energy Density (Wh/Kg)	Power Density (kW/Kg)
PANI	p only	0.7-0.8	750	400-500	8-15	1-3
PPY	p only	0.8-0.9	620	250-350	5-10	2-5
PTh	both p & n	0.8-1.0	485	80-120	20-30	5-10
PEDOT	both p & n	1.2-1.4	210	30-90	10-20	10-15

electrode material[23,33,106,109,112–114] due to good electrochemical activity, the possibility of a high degree of doping (or charging capacity), excellent stability (environmental, thermal, and electrochemical), low cost, facile synthesis, facile processing and high specific capacitance (upto 600 F/g). However, it can be reversibly doped/dedoped (charged/discharged)in the presence of protons; therefore, it requires aprotic solvent/ionic-liquid or an acidic solution for exhibiting any pseudocapacitive action. Different researchers have quoted different specific capacitance and life cycle values for PANI that can be attributed to the variation of synthesis technique, acquired morphology, oxidation state, degree of polymerization, porosity, presence of additives, the thickness of the electrode as well as measurement charge/discharge rates. For example, Li-doped PANI electrode gives a capacitance of 100 F/g and stable performance over 5000 cycles, whereas $LiPF_6$-doped PANI gives a value of 107 F/g and 9000 cycles, respectively[109]. A hybrid device using PANI cathode and carbon anode electrode combination[106] gives gravimetric capacitance of 380 F/g, stability over 4000 cycles, specific energy of 118Wh/kg, and power density ~1.25kW/kg.

Like polyaniline (PANI), polypyrrole (PPy) also displays good electroactivity, electrochemical stability, and high volumetric specific capacitance (upto 400–500 F/cm^{-3})[34,103,107]. However, the dense growth restricts the access of interior sites of the PPy chains to dopant counter-ions resulting in low gravimetric specific capacitance. The doping of PPy with bivalent counter-ions (*e.g.*, SO_4^{2-}) leads to physical cross linking of polymeric chains that causes better diffusivity and higher specific capacitance, contributed by the higher porosity. PPy has been demonstrated as an electrode in Type I supercapacitor devices and combined with poly(3-methyl thiophene)(PMeT) in Type II device architecture[107]. Ppy has also been exploited for a solid-state-supercapacitor using poly(vinyl alcohol) based electrolyte[115], with a specific capacitance of 84 F/g, good capacity retention upto 1000 cycles, and specific energy of 12Wh/kg. Ppy/polyimide (PI) combination is demonstrated to improve the charge storage properties[116] due to oxidative degradation protection of Ppy by PI, which also possesses excellent thermal stability and mechanical properties.

PTh and its analogues are another popular alternate for psudocapacitor electrodes due to p and n-doping ability, goog electrical conductivity, facile processing, good environmental stability[33,104,107,117] and chemical design flexibility to realize device voltages within the range of dielectric breakdown potentials of electrolytes. A range of p and n-dopable thiophene derivatives is given in Table 5.

It can be seen that specific capacitance in the p-doped form is generally higher than that of the n-doped state, where the poor conductivity of the n-doped form limits its utility as anode material. Some reports suggested that PTh derivatives-based Type III devices can achieve specific energy and power density values of upto 40Wh/kg and10kW/kg, respectively. The requirement of very low potentials (*i.e.*, lower than -2.0Vvs. Ag|Ag+ reference)[118,119] to realize the n-doped of PThs (poorly electrically conducting compared to p-doped form) and low stability towards oxygen and water[104], leads to the problem of high self-discharge and poor stability under repeated charge/discharge cycles. The substitution of PThs to form lower band-gap derivatives (can be n-doped at relatively lesser negative potentials) is exploited to counter the above disadvantages[104,109,110]. For example, substituting phenyl, ethyl, or alkoxy groups at the 3-position of the thiophene ring results in improved stability to oxygen and water[120] that can be further enhanced through substituents by adding electron-withdrawing groups. However, such substitution results in an escalation of materials cost along with reduced conductivity, leading to lower storage capacity and power. PMeT, a substituted polythiophene, is also exploited as electrode material[120–122] due to low cost, low resistivity[104,120], and good electrochemical stability under cyclic testing[123]. A PMeT/carbon-based hybrid device[104] displayed a gravimetric capacitance value of

Table 5 — Electrode specific capacitance and capacity from CVs at 20 mV s_1 of polymers electro-synthesized on current collectors poly(dithieno[3,4-b:3V,4V-d]thiophene) (pDTT1) and poly(3-p-fluorophenylthiophene) (pFPT)[33].

ECP	p-Doing			n-Doping		
	CV Range (V vs. SCE)	Capacitance (F/g)	Capacity (mAh/g)	CV Range (V vs. SCE)	Capacitance (F/g)	Capacity (mAh/g)
pFPT	1.0 to -0.2	95	19	-1.7 to -1.0	80	9
pDTT1	1.0 to -0.2	110	19	-1.5 to -0.2	75	17
pMeT	1.15 to -0.2	230	62	-2.0 to -1.0	165	26

220 F/g for the individual PMeT electrode (three-electrode configuration) and only 35 F/g for the final device(two-electrode configuration). Additionally, such substituted-polythiophene-based systems were highly stable with less than 0.02% capacity loss after 2000 cycles for PFPT and 0.004% after 10000 cycles for PMeT. In other works[120],the gravimetric capacitance of ~40 F/g and capacity of ~20mAh/g was achieved at a discharge current density of 5mA/cm^2 which decreases to ~30 F/g and ~8mAh/g at 40 mA/cm^2. Over the years, poly(3,4-ethylenedioxythiophene) (PEDOT) has also been exploited as a pseudocapacitive electrode because of low oxidation potential, good electrochemical activity/stability, high conductivity/mobility, good film forming ability and broad electrochemical potential window[33,107,110,117,120,124–131]. However, the low degree of doping (<0.33) and large molecular weight result in low specific capacitance (90 F/g or less)[31]. PEDOT has been exploited in symmetric supercapacitors (Type I device) as well as a PEDOT cathode/activated carbon anode-based hybrid device[37] where in a symmetric device displaying capacity of 22 F/g [for Et_4NBF_4/propylene carbonate (PC) system] and 27 F/g [for $LiPF_6$/ethylene carbonate/dimethyl carbonate (EC/DMC) system]. In contrast, the capacities of 19 F/g(in PC)and 50 F/g (in EC/DMC)[37] were observed for asymmetric devices. Analogue of PTh, *i.e*., poly(cyclopenta(2,1-b;3,4-b_-dithiophen-4-one)) (PcDT)[132] display specific capacitance value of ~70 F/g in p-as well as n-doped states with energy and power density values of 6Wh/kg and 1kW/kg respectively. Interestingly, though this device has a higher cell voltage (upto 3.0V) compared to PANI/PPY (only upto 1.0V), due to the instability of the n-doped form aerial capacitance decreases from 35 to 10mC/cm^2, even after only 20 cycles.As stated earlier, conducting polymers is cheap and light weight. They have suitable morphology, a fast doping-undoing process, and can be relatively easily manufactured into electrochemical supercapacitors. However, faradic reactions involve ingress/expelling of counter-ions that cause structural distortions, *e.g*., oxidation leads to the uptake of counter-ions by the polymer chains, whereas reduction is accompanied by the release of ions back to the electrolyte system.Consequently, the long-term electrochemical stability during prolonged cycling is a big problem that often over shadows the large puseducapacitance of CPs. For example, the PPy electrode-based device loses 50 % of the initial capacitance after 1000 cycles. In contrast, PThs show a continuous decrease in ES performance upon cycling[133,134] due to poor stability of n-doped forms. It has been suggested that nanostructuring of CPs (*e.g*., via forming nanotubes, nanofibers, or nanotubes) can improve capacitance and life cycle due to easy and fast access of charge storage sites and improved swelling characteristic of nanoparticulate networks. For example, ordered PANI nanowhiskers retain 95% capacitance after 3000 cycles[135]. Similarly, Gupta *et al*.[136] reported that electrochemically grown polyaniline nanowire arrays (Fig. 17 (a)) give specific capacitance values of ~820 F/g (at 1 mA/cm^2) and ~740 F/g (at 6 mA/cm^2). Further, it displays linear charge-discharge (within 0 to 0.7 V) characteristics with high efficiency (~99%) and no potential drop (Fig. 17(b)).

Besides, as shown in Fig. 17(c), the power density values of 16 kW/kg (energy density~70 Wh/kg) and ~2.70 kW/kg (energy density ~105 Wh/kg) were displayed were much higher than the power density of~0.9 kW/kg (energy density 110 Wh/kg) for the potentiodynamically deposited(non-nanowire structure)PANI. These films show good cyclic stability (Fig. 17(d)) with good capacitance retention (93% after 500 cycles and 99% in the subsequent 1000 cycles), which highlights the role of nanostructuring in overcoming the mechanical failures causing stress triggered by fast insertion/de-insertion of counter-ions during high rate charge-discharge cycling. The replacement of low stability n-doped CP-based negative electrode by carbon-based electrode is another strategy to counter capacity loss during charge-discharge cycling[107,121,137], *e.g*., p-doped PTh/activated carbon gives stable performance for >10000 cycles[138]. Besides, formulation of composite electrodes, *e.g*. PANI/CNT, PPY/MnO_2 electrodes, could also enhance the device stability under prolonged cycling by improving CP's chain configuration, electrical conductivity, and mechanical strength[106,116,139–142].

9.3 Transition Metal Oxides

Transition metal oxides (TMOs) are important alternative (than conjugated polymers) electrode candidates for pseducapacitors due to relatively high gravimetric capacitance (compared to carbon materials) coupled with superior electrochemical stability (compared to CPs) that allow high specific

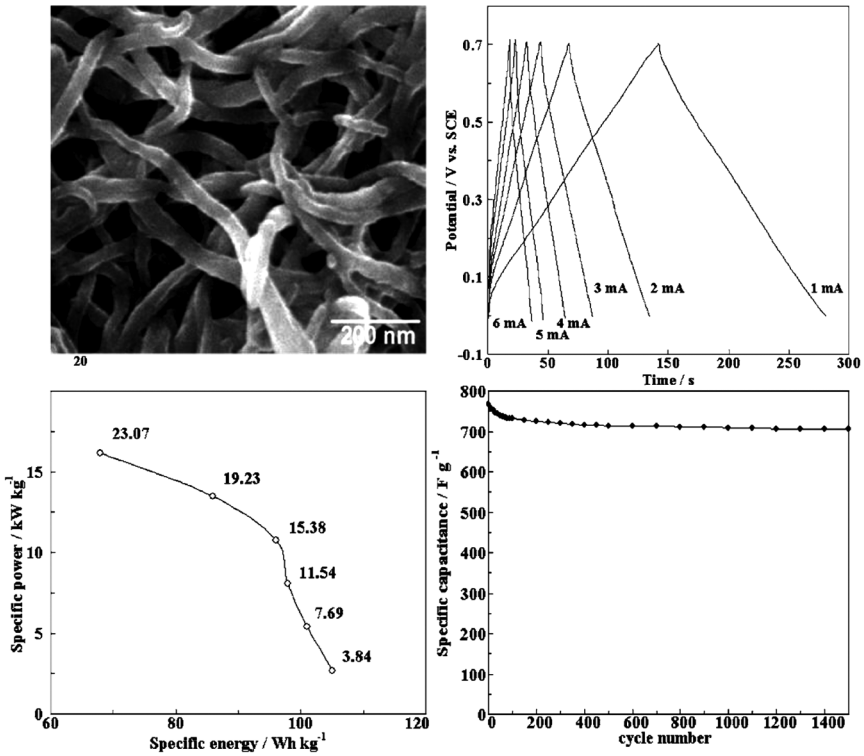

Fig. 17 — SEM images of the polyaniline nanowires, Charge/discharge cycling curves of the polyaniline nanowires at, various current densities in 1 M H_2SO_4 electrolyte.Cyclic-life data of the polyaniline nanowire capacitor. The specific capacitance was calculated for the charge-discharge cycling at the current density of 3 mA cm^{-2} in 1 M H_2SO_4 electrolyte[136], (Reprinted with the permission).

power and energy density[23]. Among the various TMOs, ruthenium oxide (RuO2) is most extensively studied due to its high specific capacitance, rate capability, good electrochemical reversibility, high conductivity, and long cycle life[14,19,20,23,46,68,124]. Its pseudo-capacitive behavior in acidic solutions is due to fast & reversible electron transfer along with the electro-adsorption of protons on the surface of RuO_2 particles. A specific capacitance value as high as 750 F/g was reported for RuO2, which, combined with low resistance, gives very high specific power. However, the rarity of ruthenium and the high cost of RuO_2 limits its commercial viability, except in the defense and aerospace sectors, where cost is not an issue.

Less expensive oxides like Mn-, Fe-, V-, Ni- and Co-oxides have also been explored as electrode material, where in the charge storage mechanism is based on the adsorption of electrolyte cations on the electrode's surface and incorporation of the proton as described below:

$$MnO_2 + xC^+ + yH^+ + (x+y)e^- \longleftrightarrow MnOOC_xH_y$$

All these compounds display pseudocapacitance due to variable oxidation states resulting in charge storage/release corresponding to oxidation/reduction reactions. The MnO_2-based electrodes exhibited specific capacitance values upto 600 F/g for thin films and 300 F/g for powder-based electrodes. In contrast, the porous MnO2 showed a specific capacitance of ~260 F/g with good stability under cyclic loading.

Nickel oxide is another potential candidate for supercapacitor electrodes with only the drawback of $Ni(OH)_2$ cathode as a decrease in specific capacitance upon increasing the current density. The nanoporous $Ni(OH)_2$ film displays a specific capacitance of ~580 F/g though long-term cyclic stability is poor, with retention of 95% capacity after 400 cycles. The electrochemically deposited NiO films with porous morphology display a pseudo-rectangular cyclic voltammogram with 87.5% capacity retention after 5000 cycles.Over the years, vanadium nitride (VN) has emerged as promising anode material for asymmetric supercapacitors (ASCs) due to large gravimetric capacitance, high electrical conductivity, and broad potential window in negative potential range. Nevertheless, its poor electrochemical stability under repeated cycling restricts its utility as electrode material. It has been demonstrated that VOx// VN-based ASC devices possess an electrochemical

window of 1.8 V with good cyclic stability and retention of more than 87% capacitance after 10000 cycles.

10 Electrolyte

The electrolyte, which typically consists of single or mixed solvents with single or multiple dissolved ionic salts in combination with an electrode material, collectively governs the performance of assembled device[14,19,23]. For example, the electrolyte plays a leading role in regulating the specific energy and power values by deciding the operating voltage and internal resistance. A large operating voltage value is expected to provide high energy/power density and good electrolyte stability in the applied potential range. The electrolyte resistance is controlled by the charge and concentration of free charge carriers and their ionic mobility. Three different types of electrolytes have been exploited as ion sources, viz. aqueous (*e.g.*, H_2SO_4, KOH, Na_2SO_4 NH_4Cl aqueous solution, *etc*.), organic (*e.g.*, acetonitrile, PC, *etc*.) and ionic liquids based electrolytes[14,19,23,49,129]. The aqueous electrolytes possess a high ionic concentration, low internal resistance, high capacitance, and power. However, their low operating voltage (upto 1.2 V, beyond which electrolytic decomposition of water takes place) limits the energy storage capacity and power deliverability. It has been shown that a comparatively higher energy density is obtained using an aprotic electrolyte than an aqueous electrolyte (Fig. 18)[143]. In contrast, an organic/non-aqueous system allows a much higher operating voltage (upto 3.5 V), making achieving high energy/power density highly probable. However, non-aqueous electrolytes have associated disadvantages such as relatively high cost, large resistance (resulting in low specific power), low dielectric constant (resulting in lower specific capacitance), environmental hazards (due to toxicity), and safety issues(due to the flammability). The current trend in supercapacitors is to shift from aqueous to non-aqueous medium and use aprotic solvents like acetonitrile or PC

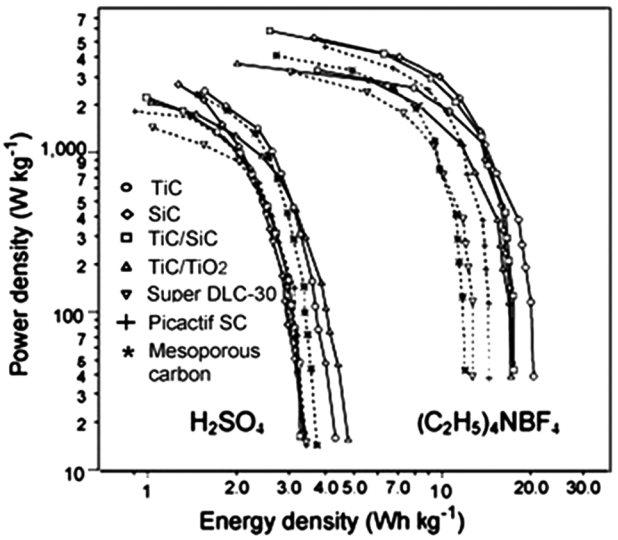

Fig. 18 — Ragone plots for comparison for the performance of various types of carbon electrodes in aqueous electrolytes and aprotic electrolytes (© Science Direct, reprinted with permission[143]).

It's worth mentioning that the high electrolyte resistance of organic electrolytes reduces the maximum power the higher operating potential partly compensates for it. Further, larger pore sizes of electrode materials are required for organic electrolytes due to the large size of organic molecules than aqueous ions. Additionally, the output voltage of organic electrolytes is extremely sensitive toward moisture content which must be kept at a very low value (<5ppm).

Ionic liquids (ILs or molten salts) are ideal electrolytes due to high ionic conductivity, low vapor pressure, non-flammability, and broad electrochemical potential window (upto 4.5 V)[23]. They are free from solvents and are composed of cations and anions of well-defined size (unsolvated), whose electrochemical stability determines their permissible voltage window. The relatively low ionic conductivity of ILsat low room temperature restricted their use preferentially at high temperatures. Again, the physico-chemical properties of these ILs depend upon the nature of cation and anion, *e.g.*, aliphatic quaternary ammonium and pyrrolidinium salts display wider electrochemical potential window and lower conductivity values than 1-ethyl-3-methylimidazolium based ILs. Supercapacitors have also been assembled using ILs in combination with carbon materials, CP, or metal oxide-based electrodes, *e.g.*, N-Butyl-N-methyl pyrrolidiniumbis-(trifluoromethane sulfonyl)imide (NBNMPBTSI) IL with activated carbon or carbide-derived carbon (CDC)/1-Ethyl3-methyl imidizolium bis (trifluoromethylsulfonyl) imide based systems. It has also been demonstrated that 1-butyl-3-methyl imidazolium hexafluorophosphate/ mesoporous nickel-based mixed rare-earthoxide hybrid device displays a power density of ~460 W/kg, the higher energy density of 50 Wh/kg, and excellent

cycle life. However, the lower conductivity of ILs compared to aprotic electrolytes result in lower power density values. Attempts have been made to improve conductivity by combining ILs with organic solvents, *e.g*., IL/PC/TEMABF4 electrolytes displayed better conductivity, higher capacitance, and enhanced power density(especially at low-temperature). However, this comes at the expense of safety (more fire hazards) and environmental issues (more toxicity).

11 Future challenges and Prospects

Recently, supercapacitors have emerged as promising energy storage alternatives with practical applicability in broad areas, *e.g*., backup power resources, pulse power for automobiles, fuel cells, and energy recovery systems in hybrid electric vehicles (HEVs). However, despite their exceptional power performance compared to batteries, the relatively lower energy density is a significant bottleneck in their commercial exploitation as energy storage systems. Therefore, the foremost challenge in realizing commercially viable and high-energy density supercapacitor is developing better electrode materials with high specific capacitance, broad potential windows, and good electrochemical stability. Though the recently exploited electrode materials (*e.g*., a carbon-based material, conducting polymers, and metal oxides) have shown some promise, they have their disadvantages. For example, despite their higher specific surface area, rational pore design, and good electrochemical stability, carbon materials still display low energy densities due to pure wettability and pore utilization. Similarly, conducting polymers with high pseudocapacitance suffered from swelling/shrinking induced mechanical degradation and thus capacity/performance loss. Likewise, though the transition metal oxides display high specific capacitances, good electrochemical/mechanical stability, and high power/energy densities, their high-cost limits commercial viability. Therefore, alternative electrode materials must be sought to overcome the above drawbacks. The crucial research directions in ES electrode development technology are hybrids/composites, nanostructured materials, and functional nanocomposites. The additive or synergistic cooperation of the composite's constituent phases may improve specific surface area/porosity, facilitate charge transport, extend the potential window, improve the mechanical strength/ cyclingstability, and contribute towards extra storage capacity via pseudocapacitance component. Similarly, the nanomaterials like nano-tubes/rods/fibers, nanoplatelets, nanospheres, or aerogels with high specific surface area, can provide short ionic transport paths and improve electrode/electrolyte contact leading to high charge/discharge capacities. In addition to electrodes, dedicated efforts are also required to develop electrolytes with wide potential windows, good electrode-wetting characteristics, and low electrochemical resistance. Particularly, ionic liquid-based electrolytes with electrochemical stability beyond 4V and very low series resistance are required to improve energy density and maintain specific power. Further, compared to other energy storage alternates, the relatively high cost of supercapacitors requires the development of low-cost technologies. It is essential to note that any effort to improve energy densities, high rate capability (*i.e*., high specific power), and good cyclic stability should not be compromised. At last, their efficiency, reliability, and safety should be improved, and environmentally friendly technologies must be adopted to develop next-generation state-of-the-art supercapacitors that can duly complement or even replace batteries in advanced electronics and HEVs.

Acknowledgment

The author would like to thank Director CSIR-NPL for the necessary support and encouragement for the work. Thanks are also due to colleagues and friends who extended valuable suggestions towards the evolution of this article.

References

1 Shaqsi A Z, Sopian K & Al-Hinai A, *Energy Rep*, 6 (2020) 288.
2 Alamri B R & Alamri A R, Technical review of energy storage technologies when integrated with intermittent renewable energy, *International Conference on Sustainable Power Generation and Supply* 1–5 (IEEE, China) 2009.
3 Chatterjee D P & Nandi A K, *J Mater Chem A,* 9 (2021) 15880.
4 Menegaki A, *Renew Sustain Energy Rev,* 12 (2008) 2422.
5 Parida B, Iniyan S & Goic R, *Renew Sustain Energy Rev,* 15 (2005) 1625.
6 Chen H, Cong T N, Yang W, Tan C, Li Y & Ding Y*, Prog Nat Sci,* 19 (2009) 291.
7 Gür T M, *Energy Environ Sci,* 11 (2018) 2696.
8 Koohi-Fayegh S & Rosen M A, *J Energy Storage,* 27 (2020) 101047.
9 Sharma P, Arora K, Tripathi A & Tripathi S K , *J Energy Storage,* 21 (2019) 801.
10 Chavan C, Bhajantri R F, Bulla S, Ravikumar H B, Raghavendra M, Sakthipandi K, Yogesh K, Prasanna B P, *Ceram Int,* 48 (2022) 17864.
11 Brindha R, Mohanraj R, Manojkumar P, Selvam M & Sakthipandi K, *J Electrochem Soc,* 167 (2020) 120539.

12 Sun J, Luo B & Huanxin L, *Adv Energy Sustain Res,* 3 (2022) 2100191.
13 Conway B E, *J Electrochem Soc,* 138 (1991) 1539.
14 Conway B E, Electrochemical Supercapacitors: Scientific Fundamentals and Technological Applications, (Spinger Link), 2002.
15 Jayalakshmi M & Balasubramanian K, *Int J Electrochem Sci*, 3 (2008) 1196.
16 Liang Y, Zhao C, Yuan H, Chen Y, Zhang W, Huang J, Yu D, Liu Y, Titirici M, Chueh Y, Yu H & Zhang Q, *Info Mat,* 1 (2019) 6.
17 Etacheri V, Marom R, Elazari R, Salitra G & Aurbach D, *Energy Environ Sci,* 4 (2011) 3243.
18 May G J, Davidson A & Monahov B, *J Energy Storage*, 15 (2018) 145.
19 Chadha N, Bhat Md Y, Hashmi S A & Saini P, *J Energy Storage,* 46 (2022) 103789.
20 Conway B E & Pell W G, *J Solid State Electrochem,* 7 (2003) 637.
21 Simon P & Gogotsi Y, *Nat Mater,* 7 (2008) 845.
22 Zhang L L & Zhao X S, *Chem Soc Rev,* 38 (2009) 2520.
23 Wang G, Zhang L & Zhang J, *Chem Soc Rev,* 41 (2012) 797.
24 Becker H E, US Pat. 2,800,616A, (to General Electric Company, a corporation of New York), 1957.
25 Rightmire R A, US Pat. 3,288,641 (to The Standard Oil Company, Cleveland, Ohio, a corporation of Ohio), 1966.
26 Boos D L, US Pat. 3,536,963 (to The Standard Oil Company, Cleveland, Ohio, a corporation of Ohio), 1970
27 Sharma P & Bhatti T S, *Energy Convers Manag,* 51 (2010) 2901. Conway B E, Birss V & Wojtowicz J, *J Power Sources,* 66 (1997) 1.
28 Rai R, *Smart materials for smart living*, Nova Science Publishers Inc, 2017.
29 Sarangapani S, Tilak B V & Chen C P, *J Electrochem Soc,* 143 (1996) 3791.
30 Kötz R & Carlen M, 45 (2000) 2483.
31 Miller J R & Burke A, *Electrochem Soc Interface,* 17(2008) 53.
32 Snook G A, Kao P & Best A S, *J Power Sources,* 196 (2011), 1.
33 An K H, Jeon K K, Heo J K, Lim S C, Bae D J & Lee Y H, *J Electrochem Soc,* 149 (2002) A1058.
34 Diederich L, Barborini E, Piseri P, Podestà A, Milani P, Schneuwly A & Gallay R, *Appl Phys Lett,* 75 (1999) 2662.
35 Qu D & Shi H, *J Power Sources,* 74 (1998) 99.
36 Frank R M, Johnson C, Owens T & Stephens B, *J Power Sources,* 47 (1994) 303.
37 Osaka T, Liu X, Nojima M & Momma T, *J Electrochem Soc,* 146 (1999) 1724.
38 Bharti, Kumar A, Ahmed G, Gupta M, Bocchetta P, Adalati R, Chandra R & Kumar Y, *Nano Express,* 2 (2021) 022004.
39 Helmholtz H, *Ann Phys Chem,* 165 (1853) 211.
40 Chapman D L, *Mag J Sci,* 25 (1913) 475.
41 Gouy M, *J Phys Théorique Appliquée,* 9 (1910) 457.
42 Grahame D C, *Chem Rev,* 41 (1947) 441.
43 Stern H O, Zeitschrift für Elektrochemie und angewandte physikalische Chemie, 30 (1924) 508.
44 Bockris J O M , Devanathan M A V & Muller K, *Proc R Soc Lond Ser Math Phys Sci,* 274 (1963) 55.
45 Jang J H, Han S, Hyeon T & Oh S M, *J Power Sources,* 123 (2003) 79.
46 Pandolfo A G & Hollenkamp A F, *J Power Sources,* 157 (2006) 11.
47 Laforgue A, Simon P, Fauvarque J F, Sarrau J F & Lailler P, *J Electrochem Soc,* 148 (2001) A1130.
48 Simon P & Gogotsi Y, *Acc Chem Res,* 46 (2013) 1094.
49 Zhang Y, Feng H, Wu X, Wang L, Zhang A, Xia T, Dong H, Li X, Zhang L, *Int J Hydrog Energy,* 34 (2009) 4889.
50 Largeot C, Portet C, Chmiola J, Taberna P-L, Gogotsi Y & Simon P, *J Am Chem Soc,* 130 (2008) 2730.
51 Rodríguez-Reinoso F & Molina-Sabio M, *Carbon*, 30 (1992) 1111.
52 Kierzek K, Frackowiak E, Lota G, Gryglewicz G & Machnikowski J, *Electrochimica Acta,* 49 (2004) 515.
53 Laine J & Yunes S, *Carbon,* 30 (1992) 601.
54 Yang H, Yoshio M, Isono K & Kuramoto R, *Electrochem Solid-State Lett,* 5 (2002) A141.
55 Raymundo-Piñero E, Kierzek K, Machnikowski J & Béguin F, *Carbon,* 44 (2006) 2498.
56 Raymundo-Piñero E, Leroux F & Béguin F, *Adv Mater,* 18 (2006) 1877.
57 Liang J, Qu T, Kun X, Zhang Y, Chen S, Cao Y-C, Xie M & Guo X, *Appl Surf Sci*, 436 (2018) 934.
58 Atika & Dutta R K, *Energy Technol,* 9 (2021) 2100463.
59 Suárez-García F, Martínez-Alonso A & Tascón J M D, *Carbon,* 42 (2004) 1419.
60 Villar-Rodil S, Denoyel R, Rouquerol J, Martínez-Alonso A & Tascón J M D, *J Colloid Interface Sci,* 252 (2002) 169.
61 Yoon S-H, Lim S, Song Y, Ota Y, Qiao W, Tanaka A & Mochida I, *Carbon,* 42 (2004) 1723.
62 Babel K & Jurewicz K, *J Phys Chem Solids,* 65 (2004) 275.
63 Baughman R H, Zakhidov A A & de Heer W A, *Science,* 297 (2002) 787.
64 Popov V, *Mater Sci Eng R Rep,* 43 (2004) 61.
65 Khan W, Sharma R & Saini P, 'Carbon Nanotube-Based Polymer Composites: Synthesis, Properties and Applications' in Carbon Nanotubes - Current Progress of their Polymer Composites , Edited by Berber M R & Hafez I H, InTech, Croatia, 2016.
66 Arepalli S, Fireman H, Huffman C, Moloney P, Nikolaev P, Yowell L, Kim K, Kohl P A, Higgins C D, Turano S P, Ready W J, *JOM*, 57 (2005) 26.
67 Qin X, Durbach S & Wu G T, *Carbon,* 42 (2004) 451.
68 Zhang H, Cao G, Wang Z, Yang Y, Shi Z & Gu Z, *Nano Lett,* 8 (2008) 2664.
69 Niu C, Sichel E K, Hoch R, Moy D & Tennent H, *Appl Phys Lett,* 70 (1997) 1480.
70 Frackowiak E, Jurewicz K, Delpeux S & Béguin F, *J Power Sources,* 97 (2001) 822.
71 Frackowiak E, Gautier S, Gaucher H, Bonnamy S & Beguin F, *Carbon,* 37 (1999), 61.
72 Signorelli R, Ku D C, Kassakian J G & Schindall J E, *Proc IEEE,* MIT Libraries, (2009) 1837.
73 Futaba D N, Hata K, Yamada T, Hiraoka T, Hayamizu Y, Kakudate Y, Tanaike O, Hatori H, Yumura M & Iijima S, *Nat Mater,* 5 (2006) 987.
74 Lee J, Han S & Hyeon T, *J Mater Chem,* 14 (2004) 478.
75 Zhang W, Cheng R, B, H, Lu Y, Ma L, & He X, *New Carbon Mater,* 36 (2021) 69.
76 Zhao X S, Su F, Yan Q, Guo W, Bao X Y, Lv L & Zhou Z, *J Mater Chem,* 16 (2006), 637.
77 Ryoo R, Joo S H & Jun S, *J Phys Chem B,* 103 (1999) 7743.
78 Ryoo R, Joo S H, Kruk M & Jaroniec M, *Adv Mater,* 13 (2001) 677.

79 Huang J, Sumpter B G & Meunier V, *Chem-Eur J,* 14 (2008) 6614.
80 Frackowiak E, *Phys Chem Chem Phys,* 9 (2007) 1774.
81 Wang D-W, Li F, Liu M, Lu G Q & Cheng H-M, *Angew Chem Int Ed,* 47 (2008) 373.
82 Ania C O, Khomenko V, Raymundo-Piñero E, Parra J B & Béguin F, *Adv Funct Mater,* 17 (2007) 1828.
83 Li W, Chen D, Li Z, Shi Y, Wan Y, Wang G, Jiang Z & Zhao D, *Carbon,* 45 (2007) 1757.
84 Yamada H, Nakamura H, Nakahara F, Moriguchi I & Kudo T, *J Phys Chem C,* 111 (2007) 227.
85 Schmitt C, Pröbstle H & Fricke J, *J Non-Cryst Solids,* 285 (2001) 277.
86 Li J, Wang X, Huang Q, Gamboa S & Sebastian P J, *J Power Sources,* 158 (2006) 784.
87 Fang B & Binder L, *J Power Sources,* 163 (2006) 616.
88 Supercapacitor: Wikipedia: https://en.wikipedia.org/wiki/ Supercapacitor.
89 Saini P & Aror M, 'Microwave Absorption and EMI Shielding Behavior of Nanocomposites Based on Intrinsically Conducting Polymers, Graphene and Carbon Nanotubes' in New Polymers for Special Applications, Edited by De Souza Gomes, A (InTech, Croatia), (2012) 71.
90 Sharma R & Saini P, Graphene-Based Composites and Hybrids for Water Purification Applications, in Diamond and Carbon Composites and Nanocomposites, edited by Aliofkhazraei, M (InTech,Croatia), (2016) 21.
91 Liu C, Yu Z, Neff D, Zhamu A & Jang B Z, *Nano Lett,* 10 (2010) 4863.
92 Stoller M D, Park S, Zhu Y, An J & Ruoff R S, *Nano Lett*, 8 (2008) 3498.
93 Lv W, Tang S-M, He Y-B, You C-H, Shi Z-Q, Chen X-C, Chen C-C, Hou P-X, Liu C & Yang Q-H, *ACS Nano*, 3 (2009) 3730.
94 Xu Y, Sheng K, Li C & Shi G, *ACS Nano*, 4 (2010) 4324.
95 Wang H, Casalongue H S, Liang Y & Dai H, *J Am Chem Soc,* 132 (2010) 7472.
96 Vivekchand S R C, Rout C S, Subrahmanyam K S, Govindaraj A & Rao C N R, *J Chem Sci,* 120 (2008) 9.
97 Zhang L L, Zhou R & Zhao X S, *J Mater Chem,* 20 (2010) 5983.
98 Si Y & Samulski E T, *Chem Mater,* 20 (2008) 6792.
99 Yan J, Wei T, Shao B, Ma F, Fan Z, Zhang M, Zheng C, Shang Y, Qian W & Wei F, *Carbon,* 48 (2010) 1731.
100 Chen S, Zhu J, Wu X, Han Q & Wang X, *ACS Nano,* 4 (2010) 2822.
101 Saini P, Fundamentals of Conjugated Polymer Blends, Copolymers and Composites, (John Wiley & Sons, Inc, USA), (2015) 3.
102 Liu P, Polypyrrole/Inorganic Nanocomposites for Supercapacitors, in Fundamentals of Conjugated Polymer Blends, Copolymers and Composites, Edited by Saini P, (John Wiley & Sons, Inc, USA), (2015) 419.
103 Laforgue A, Simon P, Sarrazin & Fauvarque J F, *J Power Sources,* 80 (1999) 142.
104 Wee B-H & Hong J-D, *Langmuir,* 30 (2014) 5267.
105 Park J H & Park O O, *J Power Sources,* 111 (2002) 185.
106 Hashmi S, *Solid State Ion,* 152 (2002) 883.
107 Rudge A, Raistrick I, Gottesfeld S & Ferraris J P, *Electrochimica Acta,* 39 (1994) 273.
108 Ryu K, *Solid State Ion,* 152–153(2002) 861.
109 Villers D, Jobin D, Soucy C, Cossement D, Chahine R, Breau L & Bélanger D, *J Electrochem Soc,* 150 (2003) A747.
110 Mastragostino M, Arbizzani C, Meneghello L & Paraventi R, *Adv Mater,* 8 (1996) 331.
111 Chen W-C & Wen T-C, *J Power Sources,* 117 (2003) 273.
112 Wu M, Snook G A, Gupta V, Shaffer M, Fray D J & Chen G Z, *J Mater Chem,* 15 (2005) 2297.
113 Sivakkumar S, *J Power Sources,* 137 (2004) 322.
114 Hashmi S A, Latham R J, Linford R G & Schlindwein W S, *Polym Int,* 47 (1998) 28.
115 Iroh J O & Levine K, *J Power Sources*, 117 (2003) 267.
116 Lota K, Khomenko V & Frackowiak E, *J Phys Chem Solids,* 65 (2004) 295.
117 Levi M D, Gofer Y, Aurbach D, Lapkowski M, Vieil E & Serose J, *J Electrochem Soc,* 147 (2000) 1096.
118 Skompska M, Mieczkowski J, Holze R & Heinze J, *J Electroanal Chem,* 577 (2005) 9.
119 Arbizzani C, Catellani M, Mastragostino M & Mingazzini C N, *Electrochimica Acta,* 40 (1995) 1871.
120 Xiao Q & Zhou X, *Electrochimica Acta,* 48 (2003) 575.
121 Balducci A, Henderson W, Mastragostino M, Passerini S, Simon P & Soavi F, *Electrochimica Acta,* 50 (2005) 2233.
122 Di Fabio A, Giorgi A, Mastragostino M & Soavi F, *J Electrochem Soc,* 148 (2001) A845.
123 Huang L-M, Wen T-C & Gopalan A, *Electrochimica Acta,* 51 (2006) 3469.
124 Vadivel M A, *J Power Sources,* 159 (2006) 312.
125 Arbizzani C, *J Power Sources,* 100 (2001) 164.
126 Arbizzani C, Balducci A, Mastragostino M, Rossi M & Soavi F, *J Power Sources,* 119 (2003) 695.
127 Ferraris J P, Eissa M M, Brotherston I D & Loveday D C, *Chem Mater,* 10 (1998) 3528.
128 Stenger-Smith J D, Webber C K, Anderson N, Chafin A P, Zong K & Reynolds J R, *J Electrochem Soc,* 149 (2002) A973.
129 Randriamahazaka H, Plesse C, Teyssié D & Chevrot C, *Electrochem Commun,* 6 (2004) 299.
130 Peng C, Snook G A, Fray D J, Shaffer M S P & Chen G Z, *Chem Commun,* 44 (2006) 4629.
131 Fusalba F, El Mehdi N, Breau L & Bélanger D, *Chem Mater,* 11 (1999) 2743.
132 Wang J, Wang C Y, Too C O & Wallace G G, *J Power Sources,* 161 (2006) 1458.
133 Wang C Y, Ballantyne A M, Hall S B, Too C O, Officer D L, & Wallace G G, *J Power Sources,* 156 (2006) 610.
134 Wang J, Too C O, Zhou D & Wallace G G, *J Power Sources,* 140 (2005) 162.
135 Gupta V & Miura N, *Electrochem Solid-State Lett,* 8 (2005) A630.
136 Yang J & Martin D C, *Sens Actuators Phys,* 113 (2004) 204.
137 Sung J H, Kim S J & Lee K H, *J Power Sources,* 124 (2003) 343.
138 Tripathi S, Kumar A & Hashmi S, *Solid State Ion,* 177 (2006) 2979.
139 Boyano I, Bengoechea M, de Meatza I, Miguel O, Cantero I, Ochoteco E, Rodr´ıguez J, Lira-Cantu M & Gómez-Romero, P, *J Power Sources,* 166 (2007) 471.
140 Garcia-Belmonte G & Bisquert J, *Electrochimica Acta,* 47 (2002) 4263.
141 Amanokura J, Suzuki Y, Imabayashi S & Watanabe M, *J Electrochem Soc,* 148 (2001) D43.
142 Fernández J A, Arulepp M, Leis J, Stoeckli F & Centeno T A, *Electrochimica Acta*, 53 (2008) 7111.